

الجمهورية الجزائرية الديمقراطية الشعبية

People's Democratic Republic of Algeria

وزارة التعليم العالي والبحث العلمي

Ministry of Higher Education and Scientific Research

جامعة غرداية

*Registration number*

University of Ghardaia



كلية العلوم والتكنولوجيا

Faculty of Science and Technology

قسم الآلية والكهروميكانيك

Department of Automatics and Electromechanics

End of study dissertation, with a view to obtaining the diploma

**Master**

Domain: Science and Technology

Sector: Automatic

Specialty: Automatic and system

**Theme**

**Modeling induction machine with intern turn  
short circuit**

**Presented by:**

**HADJADJ Ben el-Dine**

**Mohamed BAKELLI**

**Publicly supported on..... /...../.....**

**Before the jury composed of:**

<b>Mohamed ARIF</b>	<b>MAA</b>	<b>University of Ghardaia</b>	<b>President</b>
<b>Abdessalam KIFOUCHE</b>	<b>MCB</b>	<b>University of Ghardaia</b>	<b>Supervisor</b>
<b>Kada BITEUR</b>	<b>MAA</b>	<b>University of Ghardaia</b>	<b>Examiner</b>
<b>Boumedienne LAADJAL</b>	<b>MAA</b>	<b>University of Ghardaia</b>	<b>Examiner</b>
<b>Abdelmadjid KADDOUR</b>	<b>PR</b>	<b>URAER</b>	<b>Guest</b>

**Academic year 2023/2024**

## الملخص

يُعد تشخيص الأنظمة الخطية وغير الخطية مجالاً واسعاً للبحث في مجال المراقبة، حيث يُسهم في تحسين خصائص الأداء وضمان وظيفة الأنظمة المعقدة. لقد تم اقتراح عدة أساليب ومناهج لحل مشكلة التشخيص في الأبحاث العلمية. ينتشر استخدام المحركات غير المتزامن بشكل كبير في الصناعة ويُستخدم في تطبيقات متنوعة تتطلب سرعات متغيرة أو ثابتة. يُشكل عطل هذه المحركات الناتج عن دوائر القصر التي تصيب بعض اللفات جزءاً ثابتاً نسبة عالية من أسباب التعطل.

يُقدم هذا البحث تقنية لتشخيص المحركات غير المتزامن ثلاثية الطور أثناء التشغيل، حيث يُعتبر انقطاع دوائر القصر في لفات الجزء الثابت، ويتم الاقتراب من الحل باستخدام المراقبة. يتم في البداية توضيح نموذج المحرك غير المتزامن وتصميم عيوبه بشكل تآلفي يُمثلها مركبات مستقلة تطبق على النظام. تقدم هذه النهجات نموذجاً جديداً لتشخيص المحركات غير المتزامن ثلاثية الطور. يتم دمج أساليب المراقبة المبتكرة لاكتشاف العيوب باستخدام تقنيات الأنماط المنزلفة، ويتم تحديد العيوب بشكل منطقي باستخدام المعالجة المنطقية المزوجة للبيانات وأخطاء المراقبة.

وفي النهاية، تُقدم نتائج المحاكاة لحالات التشغيل السليمة (خالية من العيوب) والحالات التي تحتوي على عيوب في الجزء الثابت للمحرك باستخدام برنامج ماتلاب لعرض المحاكاة.

### الكلمات المفتاحية:

- **آلة الحث (Induction Machine):** محرك كهربائي يعمل على مبدأ الحث الكهرومغناطيسي، ويُستخدم على نطاق واسع في التطبيقات الصناعية بفضل متانته وبساطته.
- **المحرك غير المتزامن (Asynchronous Motor):** مصطلح آخر لمحرك الحث، لا يتطلب التزامن مع تردد التيار الكهربائي المزود.
- **تشخيص الأعطال (Fault Diagnosis):** عملية تحديد مواقع الأعطال أو العيوب في النظام لضمان التشغيل السليم ومنع الفشل.
- **العضو الثابت (Stator):** الجزء الثابت في آلة الحث الذي يحتوي على ملفات وينتج مجالاً مغناطيسياً عندما يمر التيار خلاله.
- **العضو الدوار (Rotor):** الجزء الدوار في آلة الحث الذي يدور استجابةً للمجال المغناطيسي الذي يُنشئه العضو الثابت.
- **الدائرة القصيرة (Short Circuit):** عطل كهربائي يحدث عندما تتصل أجزاء غير مرغوبة من الدائرة، مما يسمح بمرور تيار زائد يمكن أن يتسبب في تلف.
- **المحاكاة (Simulation):** استخدام نماذج حسابية لمحاكاة سلوك نظام معين، مثل آلة الحث، تحت ظروف مختلفة للتحليل والاختبار.
- **ماتلاب (MATLAB):** لغة برمجة عالية المستوى وبيئة للحوسبة العددية والمحاكاة، تُستخدم بشكل شائع في الهندسة والبحث العلمي.
- **تقنيات المراقبة (Monitoring Techniques):** طرق وأدوات تُستخدم لمراقبة أداء النظام واكتشاف الأعطال والخلل.
- **تحويل بارك (Park Transformation):** تقنية رياضية تُستخدم لتبسيط تحليل الأنظمة الكهربائية ثلاثية الطور بتحويلها إلى نظام إحداثيات ثنائي المحاور.
- **تقنيات الانزلاق (Sliding Mode Techniques):** طرق تحكم تُستخدم لضمان استقرار النظام وأدائه رغم عدم اليقين والاضطرابات، وتُطبق غالباً في كشف الأعطال وتشخيصها.
- **كشف الأعطال (Fault Detection):** عملية تحديد وجود عطل أو حالة غير طبيعية في النظام، وتُعتبر خطوة تمهيدية قبل التشخيص.
- **العزم الكهرومغناطيسي (Electromagnetic Torque):** العزم الناتج عن تفاعل الحقول المغناطيسية للعضو الثابت والدوار في آلة الحث، مما يؤدي إلى دورانها.
- **السرعة الميكانيكية (Mechanical Speed):** سرعة دوران العضو الدوار في آلة الحث، وتقاس عادةً بالدورات في الدقيقة (RPM).
- **المحركات ثلاثية الطور (Three-phase Motors):** محركات كهربائية تُشغّل بواسطة تيار متناوب ثلاثي الطور، معروفة بكفاءتها وتُستخدم بشكل شائع في التطبيقات الصناعية.

## résumé

Le diagnostic des systèmes linéaires et non linéaires est un vaste domaine de recherche en surveillance, contribuant à améliorer les performances et à garantir le bon fonctionnement des systèmes complexes. Plusieurs méthodes et approches ont été proposées pour résoudre le problème du diagnostic dans la recherche scientifique. Les moteurs asynchrones sont largement utilisés dans l'industrie et sont appliqués dans diverses applications nécessitant des vitesses variables ou constantes. Les pannes de ces moteurs dues à des courts-circuits affectant certains enroulements représentent une part importante des causes de défaillance.

Cette recherche propose une technique de diagnostic des moteurs asynchrones triphasés en fonctionnement, en considérant les courts-circuits dans les enroulements du stator, et approche la solution par la surveillance. Tout d'abord, le modèle du moteur asynchrone et la conception de ses défauts sont présentés de manière cohérente sous forme de composants indépendants appliqués au système. Ces approches proposent un nouveau modèle de diagnostic des moteurs asynchrones triphasés. Des techniques de surveillance innovantes sont intégrées pour détecter les défauts en utilisant des techniques de glissement de mode, et les défauts sont logiquement identifiés en utilisant un traitement logique des données et des erreurs de surveillance.

Enfin, les résultats de la simulation des conditions de fonctionnement normales (sans défaut) et des conditions présentant des défauts dans le stator du moteur sont présentés en utilisant le programme Matlab pour visualiser la simulation.

### Mot-clé :

- **Machine asynchrone (Induction Machine) :** Moteur électrique fonctionnant sur le principe de l'induction électromagnétique, largement utilisé dans les applications industrielles pour sa robustesse et sa simplicité.
- **Moteur asynchrone (Asynchronous Motor) :** Autre terme pour désigner une machine asynchrone, qui ne nécessite pas de synchronisation avec la fréquence du courant d'alimentation.
- **Diagnostic des défauts (Fault Diagnosis) :** Processus d'identification et de localisation des défauts ou anomalies dans un système pour assurer un fonctionnement correct et prévenir les défaillances.
- **Stator (Stator) :** Partie fixe d'une machine asynchrone contenant les enroulements qui génèrent un champ magnétique lorsqu'un courant y circule.
- **Rotor (Rotor) :** Partie rotative d'une machine asynchrone qui tourne sous l'effet du champ magnétique produit par le stator.
- **Court-circuit (Short Circuit) :** Défaut électrique où des connexions non intentionnelles permettent au courant de contourner la charge normale, provoquant un flux de courant excessif.
- **Simulation (Simulation) :** Utilisation de modèles computationnels pour reproduire le comportement d'un système, comme une machine asynchrone, dans diverses conditions à des fins d'analyse et de test.
- **MATLAB (MATLAB) :** Langage de programmation de haut niveau et environnement pour le calcul numérique, la simulation et la visualisation de données, souvent utilisé en ingénierie et en recherche scientifique.
- **Techniques de surveillance (Monitoring Techniques) :** Méthodes et outils utilisés pour observer et suivre les performances et l'état d'un système afin de détecter les défauts et les anomalies.

- **Transformation de Park (Park Transformation) :** Technique mathématique utilisée pour simplifier l'analyse des systèmes électriques triphasés en les transformant en un système de coordonnées à deux axes.
- **Techniques de mode glissant (Sliding Mode Techniques) :** Méthodes de contrôle utilisées pour garantir la stabilité et les performances d'un système malgré les incertitudes et les perturbations, souvent appliquées à la détection et au diagnostic des défauts.
- **Détection des défauts (Fault Detection) :** Processus permettant d'identifier la présence d'un défaut ou d'une condition anormale dans un système, souvent une étape préliminaire avant le diagnostic.
- **Couple électromagnétique (Electromagnetic Torque) :** Couple produit par l'interaction des champs magnétiques du stator et du rotor dans une machine asynchrone, entraînant sa rotation.
- **Vitesse mécanique (Mechanical Speed) :** Vitesse de rotation du rotor dans une machine asynchrone, généralement mesurée en tours par minute (RPM).
- **Moteurs triphasés (Three-phase Motors) :** Moteurs électriques alimentés par un courant alternatif triphasé, connus pour leur efficacité et largement utilisés dans les applications industrielles.

# Abstract

The diagnosis of linear and nonlinear systems is a vast field of research in monitoring, contributing to the improvement of performance characteristics and ensuring the functionality of complex systems. Several methods and approaches have been proposed to solve the diagnostic problem in scientific research. Asynchronous motors are widely used in the industry and are applied in various applications requiring variable or constant speeds. The failure of these motors due to short circuits affecting some windings represents a significant portion of the causes of failure.

This research proposes a technique for diagnosing three-phase asynchronous motors during operation, considering short circuits in the stator windings, and approaches the solution through monitoring. Initially, the model of the asynchronous motor and the design of its faults are coherently presented as independent components applied to the system. These approaches propose a new model for diagnosing three-phase asynchronous motors. Innovative monitoring techniques are integrated to detect faults using sliding mode techniques, and faults are logically identified using logical data processing and monitoring errors.

Finally, the simulation results for normal operating conditions (fault-free) and conditions with faults in the motor stator are presented using Matlab software to display the simulation.

## The Keywords :

- **Induction machine:** An electric motor that operates on the principle of electromagnetic induction, widely used in industrial applications for its robustness and simplicity.
- **Asynchronous motor:** Another term for an induction motor, which does not require synchronization with the supply current's frequency.
- **Fault diagnosis:** The process of identifying and locating faults or defects in a system, such as an induction machine, to ensure proper operation and prevent failures.
- **Stator:** The stationary part of an induction machine that contains windings and produces a magnetic field when current flows through it.
- **Rotor:** The rotating part of an induction machine that turns in response to the magnetic field generated by the stator.
- **Short circuit:** An electrical fault where unintended connections allow current to bypass the normal load, causing excessive current flow and potential damage.
- **Simulation:** The use of computational models to replicate the behavior of a system, such as an induction machine, under various conditions for analysis and testing.
- **MATLAB:** A high-level programming language and environment used for numerical computing, simulations, and data visualization, often employed in engineering and scientific research.
- **Monitoring techniques:** Methods and tools used to observe and track the performance and condition of a system, helping to detect faults and anomalies.
- **Park transformation:** A mathematical technique used to simplify the analysis of three-phase electrical systems by transforming them into a two-axis coordinate system.
- **Sliding mode techniques:** Control methods used to ensure the stability and performance of a system despite uncertainties and disturbances, often applied in fault detection and diagnosis.

- **Fault detection:** The process of identifying the presence of a fault or abnormal condition in a system, often a preliminary step before diagnosis.
- **Electromagnetic torque:** The torque produced by the interaction of the magnetic fields of the stator and rotor in an induction machine, causing it to rotate.
- **Mechanical speed:** The rotational speed of the rotor in an induction machine, typically measured in revolutions per minute (RPM).
- **Three-phase motors:** Electric motors powered by a three-phase alternating current (AC) supply, known for their efficiency and commonly used in industrial applications.

## Dedications

We would like to express our deepest gratitude to our families and friends for their unwavering support, encouragement, and love throughout this journey. Your belief in us has been a source of strength and inspiration.

A special thanks to our supervisor, “ABDESSALAM KIFOUICHE”, for his invaluable guidance, patience, and expertise in helping us write our graduation note. Your dedication to our success has made this achievement possible.

### Dedication Ben el Dine:

I want to thank my family especially my mom for her support ,guidance my friends and my loved ones Anfel, Mustafa, Amour, and Amine , Hicham for being there for me.

Thank you all for being an essential part of this accomplishment.

## Table of Contents

### Contents

المُلخَص .....	2
résumé .....	3
Abstract .....	5
Dedications .....	7
The Keywords : .....	9
LIST OF TABLES, GRAPHICS, AND ILLUSTRATIONS .....	10
General Introduction .....	13
Chapter I .....	15
Constitution and Representation of Induction machine faults .....	15
I.1. Introduction.....	1
I.2. The Constitution of the induction machine.....	1
I.3-Faults in an Induction Motor .....	4
I.4-Fault Types .....	4
I.5 Statistical analyses of faults: .....	8
I.6-Diagnosis of induction machine .....	8
I.7-Generality and definition.....	8
I.8-induction machine operating Modes .....	9
I.9-Fault diagnosis methods.....	9
I.10- Diagnostic techniques used to find problems with induction machines.....	10
Conclusion .....	15
ChapterII .....	16
Modeling Of Induction Machine.....	16
II.Introduction.....	17
II.1Modeling of the healthy asynchronous machine:.....	17
II.2. Modeling Without Fault .....	17
II.3. Modeling With Fault .....	23
Conclusion .....	28
ChapitreIII.....	29
Fault Detection Using d-q Analysis.....	29
III.Introduction.....	30
III.1- Simulation of an induction machine without faults.....	30
III.2- Simulation of an induction machine with faults .....	42
Conclusion .....	47
General Conclusion .....	48
References .....	50
Appendix A .....	53



<b>Appendix B</b> .....	<b>55</b>
<b>Appendix C</b> .....	<b>56</b>
<b>Appendix D</b> .....	<b>57</b>

## LIST OF TABLES, GRAPHICS, AND ILLUSTRATIONS

Figure I,1 induction machine

Figure I,2 The Stator

Figure I,3 Wound Rotor

Figure I,4 Squirrel Cage rotor

Table I,1 Classification of faults according to their origins

Figure I,5 Diagram of eccentricity faults

Figure I,6 Constitution of bearing

Figure I,7 Example of damage Caused by stator intern-turn short-circuits faults

Figure I,8 The Different stator faults

Figure I,9 Cage rotor faults (a) broken bars (b) broken intern-turn short-circuits ring

Table I,2 statistical analyses of faults in induction machine

Figure I,10 Classification of diagnostic methods

Figure I,11 Process for identifying and locating faults

Figure I,12 Structure of the stator (a) and rotor (b)

Figure II.1 Model of a three-phase induction machine

Figure II.2 Representation of induction machine

Figure II.3 Park transform illustration

Figure III.1 the supply voltage in the three-phase (a)

Figure III.2 the supply voltage in the two-phase (b)

Figure III.3 Evolution of currents in the three-phase (a)

Figure III.4 Evolution of currents in the two-phase (b)

Figure III.5 Evolution of direct (a) currents

Figure III.6 Evolution of quadratic (b) currents

Figure III.7 phase plane of direct and quadrature currents

Figure III.8 Rotor flow in both frames

Figure III.9 induction machine's rotor flow in the park frame

Figure III.10 The Evolution of electromagnetic torque

Figure III.11 The Evolution of mechanical speed

Figure III.12 Evolution of imbalanced voltages

Figure III.13 Current in park

Figure III.14 Evolution of torque (a)

Figure III.15 Evolution of speed (b)

Figure III.16 Function  $I_{sd}=f(i_{sq})$  under various voltage imbalance situations

Figure III.17 Electromagnetic Couple

Figure III.18 (a) mechanical speed , (b) Zoom speed

Figure III.19 Phase A stator current.

## List of Symbols and Abbreviations

IN: INDUCTION MACHINE

$[R_S]$ ,  $[R_r]$  : Stator and rotor resistance matrices.

$[\Phi_s]$ ,  $[\Phi_r]$ : Stator and rotor flows.

$[I_s]$ ,  $[I_r]$  : Stator and rotor currents.

$[U_s]$ ,  $[U_r]$  : Stator and rotor voltages.

$[L_s]$ ,  $[L_r]$ : Matrices of stator and rotor inductances.

$[M_{sr}]$ ,  $[M_{rs}]$ : Matrices of stator-rotor and rotor-stator mutual inductances.

$[P(Y)]$ : Park transformation matrix.

$[I_{sdq}]$ ,  $[\Phi_{rdq}]$ : Stator currents and rotor fluxes in Park.

J: Moment of inertia of the rotor.

D,Q : direct and quadratic

$f_v$ : Coefficient of viscous friction.

$T_l$ : Load torque.

$\Omega$ : Mechanical speed of the rotor.

$n_{cca}$ ,  $n_{ccb}$ ,  $n_{ccc}$  : meaning the number of short-circuited turns per phase.

$n_s$  : Total number of turns per phase.

$n_a$ ,  $n_b$ ,  $n_c$ : Ratio of the number of turns in short circuit to the total number of turns.

$f_a$ ,  $f_b$ ,  $f_c$  : Turn ratio still in function.

# General Introduction

Asynchronous machines, especially asynchronous motors (MAS), are certainly the most frequently used electrical machines in industry given their great robustness, their ease of starting, and their low maintenance prices. All these qualities justify the industry's renewed interest in this type of machine. However, these MAS motors are subjected during their operation to several constraints of different natures (electrical, magnetic, mechanical and thermal) which causes electrical or mechanical defects in the stator, or the rotor, or both at the same time. Please note that these defects can cause a shutdown leading to loss of production and costly repairs, and can even lead to deterioration of the machine.

Unfortunately, diagnosis becomes more challenging as a result of new limitations and the incorporation of these machines into increasingly intricate energy conversion systems.

Numerous diagnostic techniques exist [1]. The strategy that is chosen depends on both the complexity of the system and the knowledge that the person wants to gain about it. As a result, the discipline of electrical engineering diagnostics uses two sizable families of procedures: model-free diagnostic approaches and hardware redundancy [2]. and techniques that rely on analytical redundancy or analytical models [3, 4].

Models without any techniques rely on analyzing measured signals to obtain information. Meaningful information concerning problems can be obtained via measurable signals, such as currents, voltages, speed, vibrations, temperature, and noise emissions. Designing monitoring systems or effective diagnostic algorithms is made possible by the application of decision-making techniques (such shape recognition) based on these quantities that are typical of electrical machine functioning. The accuracy of the measurement analysis and the applicability of the fault indicators employed have a direct bearing on how well these methods work.

Analytical model-based methods rely on employing observation algorithms to keep an eye on the machine's parameters and quantities. By examining the evolution of the difference between the model and the actual process, they are able to identify failures. A number of approaches can be proposed for the detection and isolation of faults in linear or non-linear systems [13, 14]. These approaches include methods for estimating parameters [2, 4], methods based on the use of observers [6, 7, 8, 9], and methods based on the parity space [10, 11, 12]. There are other approaches as well, but these three are among the most significant.

Asynchronous machine faults can be found and isolated using a variety of techniques. Model-free (measurement-based) approaches include the so-called Park vector method [15, 16], spectral analysis of stator currents [17, 18], symmetrical component [19], etc. The creation of a set of defect indicator

signals known as residuals is the foundation of methods based on an understanding of the mathematical model. Any irregularity in the asynchronous machine's functioning can be found and interpreted through the analysis of the latter. The key components of these techniques are parameter estimation [20,21], projection onto parity space [22], and the observer approach [22,23].

The focus of the current work is on a diagnostic technique for stator intern-turn short defects, such as a decrease in turns in one or more asynchronous machine's stator phases. We outline the components of the asynchronous machine, as well as its flaws and troubleshooting techniques. modeling with the existence of stator intern-turn short faults and modeling without faults, as well as synthesizing an indirect vector control with flux direction.

The three main chapters of this dissertation are as follows:

The first introduces the components of the asynchronous machine's functioning, defects, statistics, and diagnostic techniques. In the second chapter, modeling without and with defects is carried out with a synthesis of flow orientation vector control based on the model without defects. The last chapter is devoted to the generation of residues.

# **Chapter I**

## **Constitution and Representation of Induction machine faults**

## I.1. Introduction

On induction machines, numerous malfunctions may occur. They may be magnetic, mechanical, or electrical. There are many different reasons behind them. We describe the system under study in this chapter, which in our instance is restricted to the induction machine. We start this presentation by going over the components that make up this machine. We will be particularly interested in being ready for the actual manufacturing of stator windings in this sense. Following an investigation of the various defects that could arise on each of them, let's discuss their causes and examine how these flaws affect the machine's behavior.

## I.2. The Constitution of the induction machine

Induction motor is a type of electric motor widely used in various applications due to its simplicity, reliability, and robustness (**Figure. I.1**).

The fundamental elements of an induction machine include:

**The stator:** Which is the stationary part composed of magnetic sheet discs containing windings that induce magnetism in the air gap.

**The rotor:** The rotating component consisting of magnetic sheet discs stacked along the machine's shaft, housing wound or injected windings.

**The Bearing:** Mechanical parts facilitating rotor rotation and the up-keep of various subcomponents.

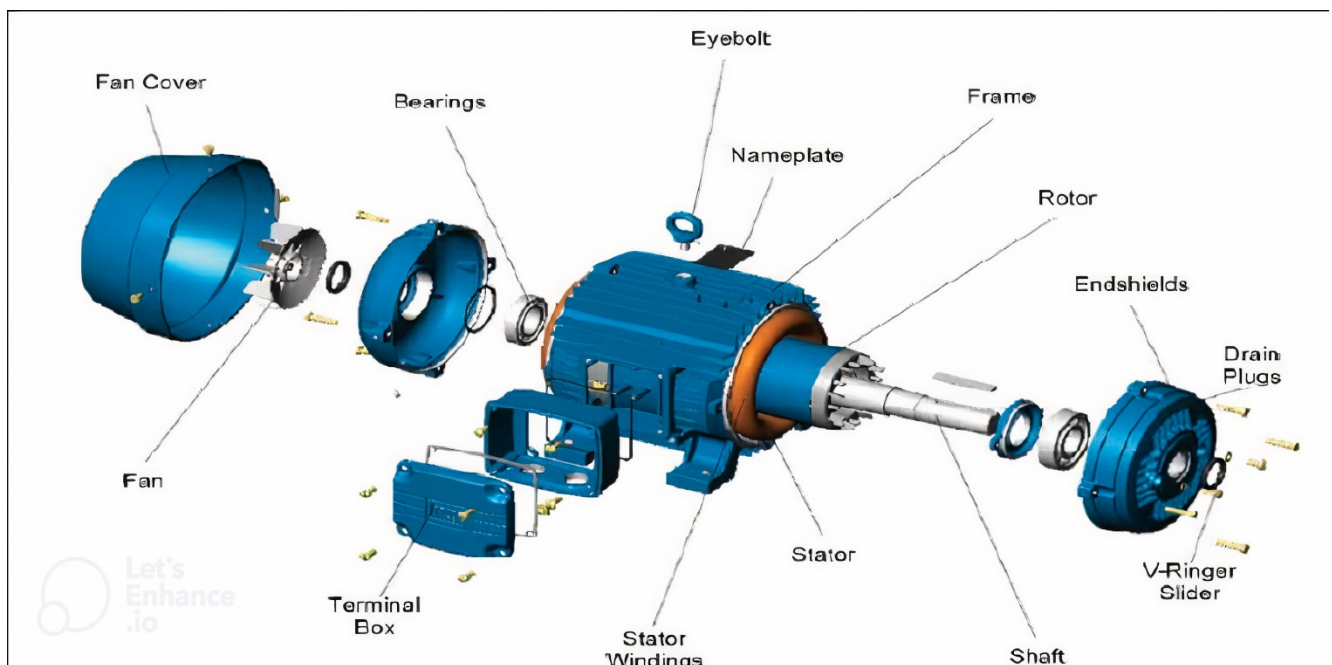


**Figure I.1:** Induction Machine.



### I.2.1. The stator:

It consists of a wound coil that is spread out within slots located in the magnetic structure. This structure comprises a series of sheets stacked together, with grooves cut parallel to the machine's axis (Figure I.2).

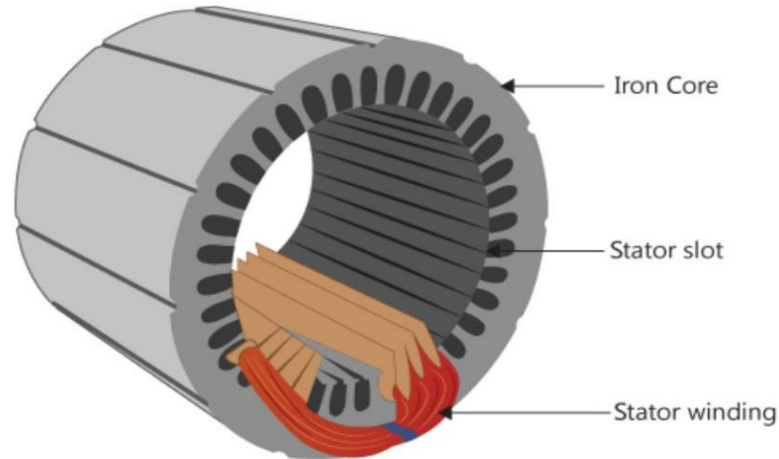


Figure I.2: The stator

### I.2.2. The Rotor:

The rotor is the moving component within an Induction Motor, situated inside the stator. An air gap separates the stator and rotor, enabling the rotor to rotate without any physical contact with the stator. There are two types of Rotors:

### I.2.3. Wound Rotor:

It consists of three-phase winding in the rotor; Rotor windings are uniformly distributed and connected in (star or Y) shape. The ends of windings are brought out at both ends and connected to the slip rings; the rheostats are connected between the slip rings and the winding ends (Figure. I.3).

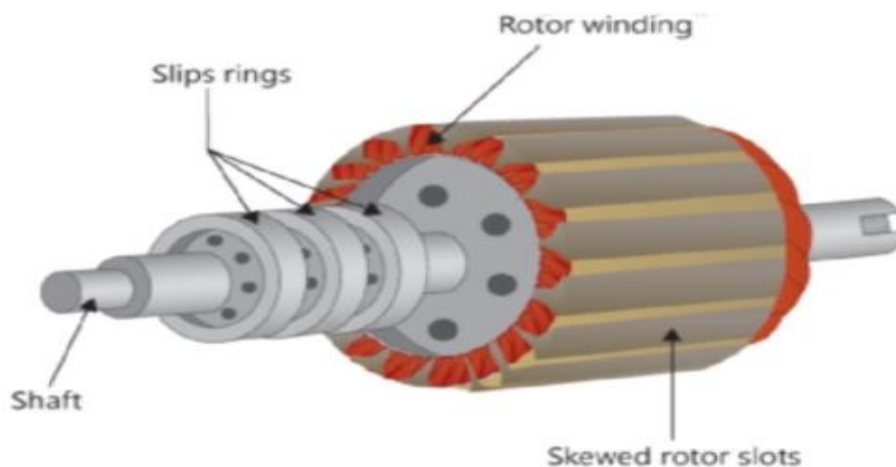
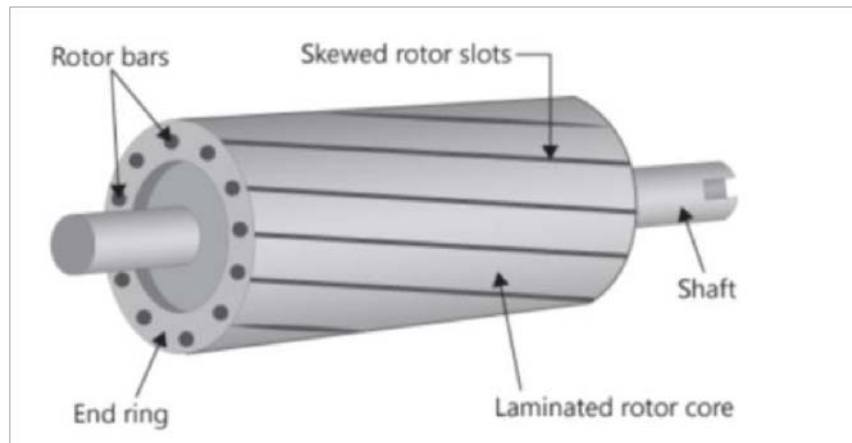


Figure I.3: Wound Rotor.

### I.2.4 Squirrel cage rotor:

It consists of copper or aluminum bars embedded in the semi-closed slots resembling a squirrel cage. The rotor slots in this type of rotor are not parallel to the shaft instead they are skewed for obtaining a quick and smooth operation. The rotor bar is connected at both the ends and short-circuited by solid rings made of copper, brass, or aluminum. Mostly used in single phase induction motor (Fig.1.4).



**Fig. I.4.:** Squirrel cage rotor

### I.2.5 The Bearings

The mechanical elements that guarantee the rotor's concentricity with respect to the stator are the bearings. When the rotor rotates, the bearings which are either positioned at the end of the shaft or housed within the bearings help to lower friction. They consist of the assembly that the flanges and bearings form. The shaft is where the bearings are installed. For concentric location on the crankcase, the outer edges of the cast iron flanges are machined. In order to accept the bearings' outer races, they are also machined on the inside edges. The flanges are fastened to the casing with bolts or clamping rods once the rotor has been positioned inside the stator with the previously mounted bearings in place.

**Table I.1:** Classification of Faults according to their origins.

Faults of induction machine	Internal	Mechanical	Contact between stator and rotor
			Bearing failure
			Eccentricity
			Movement of windings and sheets
		Electrical	Insulation failure
			Bar break
	Failure in the magnetic circuit		
	External	Mechanical	Oscillating load
			Machine overload
			Assembly fault
		Environmental	Humidity
			Temperature
			Cleanliness
		Electrical	Voltage fluctuation
			Sources of unbalanced tensions
Noisy network			

### I.3-Faults in an Induction Motor

The asynchronous machine is considered robust but can be subject to constraints during its operation: length of time, harsh conditions, which causes its failure. The main faults of the asynchronous machine can be categorized into two types: mechanical and electrical. The sources of machine faults can be internal, external or due to the environment. presents the fault tree of the asynchronous machine where the faults are classified according to their location: rotor and stator [39].

### I.4-Fault Types

The majority of surveys on electrical rotating machine failures show that bearing and stator winding failures often account for the majority of failures, with rotor winding issues being less common. [Benbouzid 2000]

#### I.4.1: Eccentricity Faults

The air gap flux density varies as a function of the air gap length. Electrical effects are felt on the stator windings. The present spectrum then shows these impacts.

Three cases of eccentricity [43]:

- Static eccentricity: Despite being displaced from the stator bore's center, the rotor still revolves around its axis.
- Dynamic eccentricity: although the rotor is centered in the bore, it is no longer able to revolve around its axis.
- A worldwide kind of eccentricity that combines the two earlier examples. The static and dynamic eccentricity are shown as follows in (Figure 1.5):

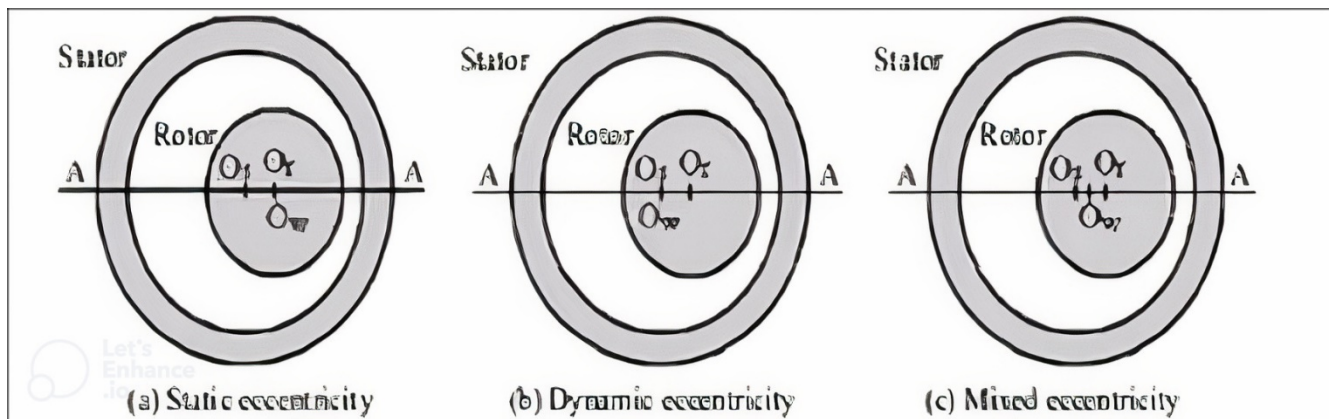


Figure I.5 Diagram of eccentricity faults

#### I.4.2. Bearing faults

Ball bearings consist of two rings, outer and inner, between which there is a set of rotating balls or rollers (Figure I.6) [40].

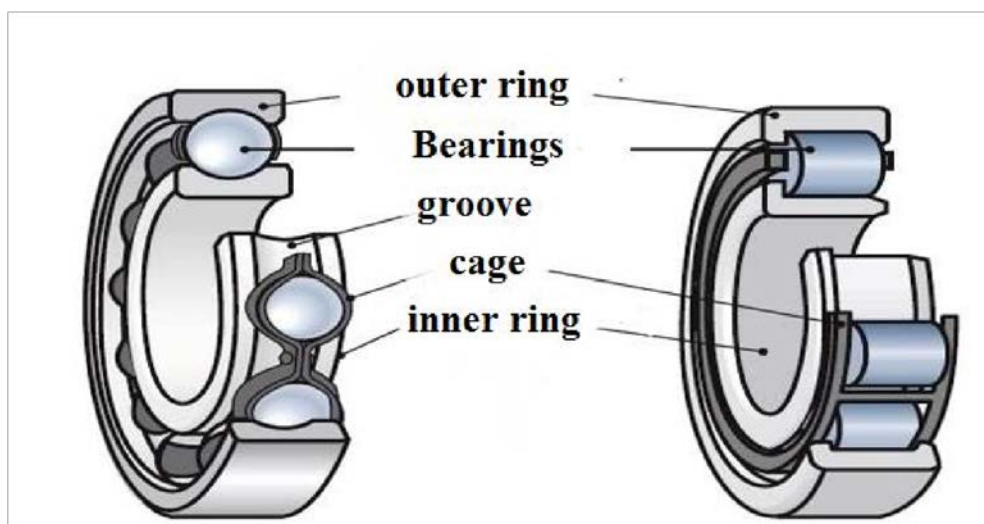


Figure I.6 Constitution of a bearing.

We can distinguish the following types of defects [41]:

- Outer ring fault.
- Inner ring fault.
- Ball fault.

### I.4.3 -intern-turn Short circuit faults:

Stator phase intern-turn short-circuits faults are known to occur in two types:

1. intern-turn short-circuits between the stator phases' turns: this kind can be divided into two groups:

The defect examined in this dissertation is the reduction of stator turns.

In the case where each of the three stator phases has  $N_s$  turns, the reduction fault of  $N_{cc}$  turns would be a total intern-turn short-circuit. This means that each short-circuited turn is linked to a place, typically a hot spot between two or more following turns, suggesting that the varnish has been destroyed. Over time, the amount of reduced rotations rises and poses a risk to both the machine and the power source.

intern-turn short-circuits exhibiting the look of an effective coil: this kind of intern-turn short-circuits involves multiple turns. the same reasons as the fault in turn reduction.

2. intern-turn short-circuits between the rotor and shell of the stator or between the turns and the casing: this kind of issue can also arise from the machine overheating, which breaks the insulation between the turns and the casing.

#### I.4.3.1 Stator faults:

The degradation of the electrical insulation generates intern-turn short-circuits faults illustrated by (Figure.

1.7). We can clarify the different possible intern-turn short-circuits faults by [38], [41]:

Intern-turn defects which appear inside the stator slots.

Faults between a phase and neutral.

Faults between a phase and the metal frame of the machine or between two stator phases.

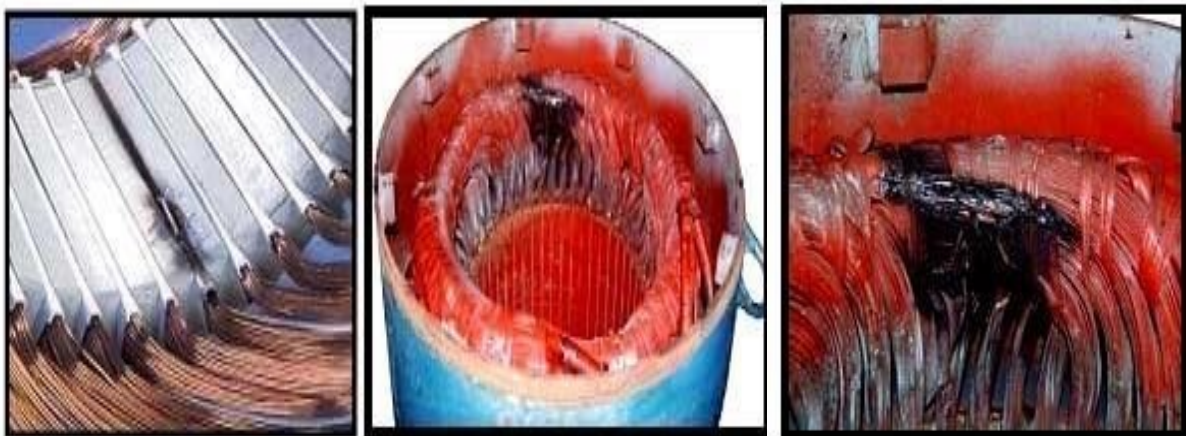


**Figure I.7** Example of damage caused by stator intern-turn intern-turn short-circuits faults

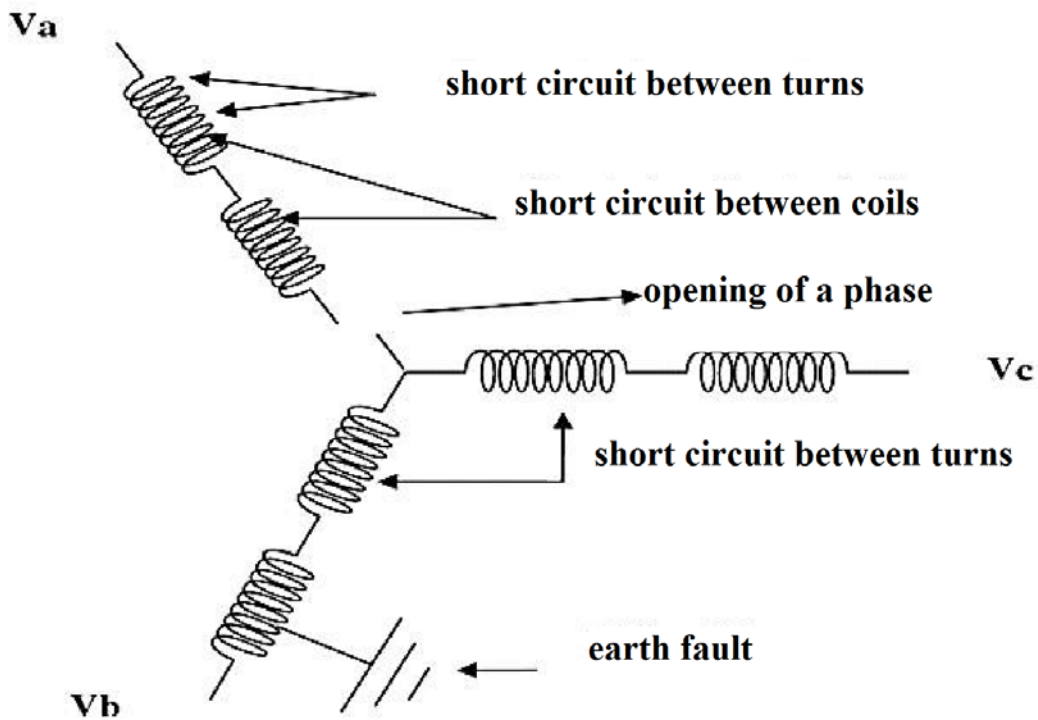


**Figure I.8** The different stator faults

**I.4.3.2 Rotor defects:**

**I.4.3.2.1 Breakage of bars:**

Bar breakage is one of the most common rotor defects (Figure I.9). A broken bar means that the current in this bar is zero [40]. The deterioration of the bars reduces the average value of electromagnetic torque and increases the amplitude of the oscillation, which causes mechanical vibrations and abnormal operation of the machine [41].

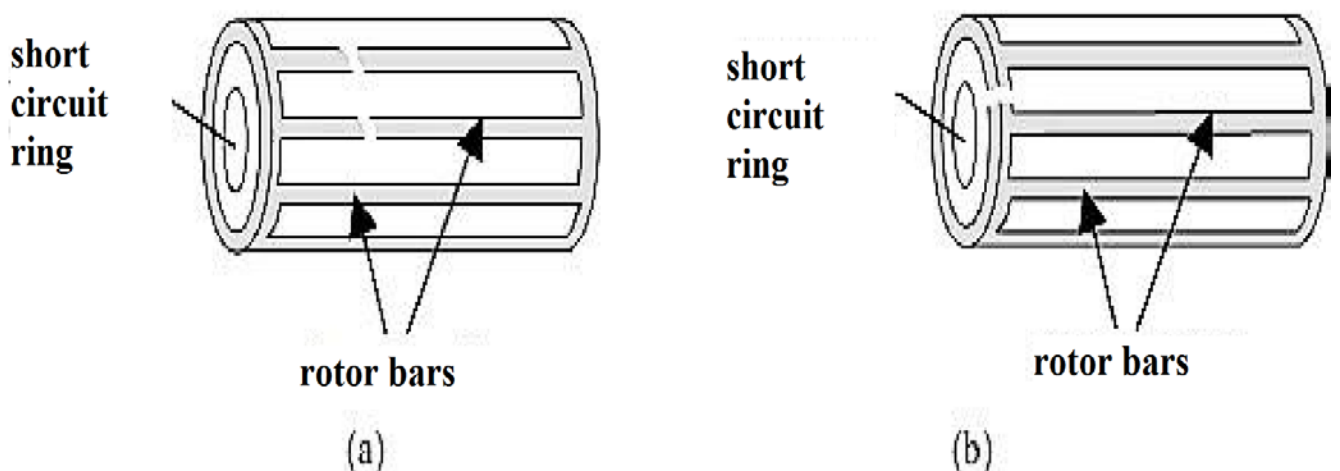


**Figure I.9** Cage rotor faults: (a) broken bars (b) broken intern-turn short-circuits ring



#### **I.4.3.2.1. Ring breaks:**

Fractures can be due to casting bubbles or differential expansions between the bars and the rings (Figure I.9). The breakage of a portion of the ring unbalances the distribution of currents in the rotor bars and therefore generates an amplitude modulation effect on the stator currents similar to that caused by the breakage of bars [41].

#### **I.5 Statistical analyses of faults:**

An Overview of multiple statistical studies on asynchronous machine failures, derived from various surveys, is provided in reference [29]. The findings apply to machines under many usage scenarios and power ranges. The distribution of failures at each subsystem level is shown in Table below. Table I.2 [23].

Sub-System	Investigation 1,2,3	Investigation 4	Investigation 5
Stator	26%	37%	15.76%
Rotor	8%	10%	7.14%
Bearings	44%	41%	51.07%
Others	22%	12%	26.03%

**Table I.2:** Statistical analyses of faults in induction machine

This table makes it evident that the majority of defects are at the bearing level, with faults at the stator level typically leading to intern-turn intern-turn short-circuits coming in second. These studies focus on equipment utilized in various operational scenarios.

#### **I.6-Diagnosis of induction machine**

In order to monitor the induction machine, the diagnostic function's goal is to identify and track down the root causes of malfunctions. It is guaranteed by the examination of a malfunction state; the diagnostic is in charge of identifying the malfunction that is the source of the problem. It is challenging to fix this issue. In fact, while it may be simple to forecast the breakdown that will occur from a particular defect, it is far more challenging to identify the fault based on its effects. Generally speaking, a failure can be attributed to multiple errors. The next step is to compare the analyses in order to offer the most appropriate explanation.

#### **I.7-Generality and definition**

Fault: its an action, voluntary or not that leads to an incorrect consideration of a restriction or direction stated in the specifications.

A fault is the discrepancy between a system parameter's nominal and actual values. Degradation: is the inability of a system to perform one of its functions as intended. Failure: is defined as a change or cessation in an assembly's capacity to carry out the necessary function or functions with the performance specified in the technical standards. Three classes can be used to categorize defects based on their severity:

Critical: necessitates immediate action.

Important: necessitates a procedure for processing.

Absorbable: initially disregarded.

Error: A component of the system that does not, or does not fully, match the requirements. It makes sense that an error results from a mistake.

Breakdown: is the incapacity of an entity (system or component) to carry out a necessary task.

Residue: This signal is intended to serve as a warning flag for irregularities in behavior or function.

### **1.8-induction machine operating Modes**

Generally speaking, an induction machine can operate in three modes:

Nominal mode: this is the state in which the machine operates in accordance with the manufacturer's specifications and completes the intended task, fulfilling its mission.

degraded mode : the machine operates at a reduced capacity; in other words, it has sustained damage but has not failed.

Failure mode: this refers to machine malfunctions, meaning a failure that occurred either suddenly or following degradation. Effects that may be quantitative or measured define a failure mode.

### **I.9-Fault diagnosis methods**

A wide range of diagnostic methods are used in defect detection. They are in line with the variety of issues that are faced. They can be categorized in the following figure based on their types.



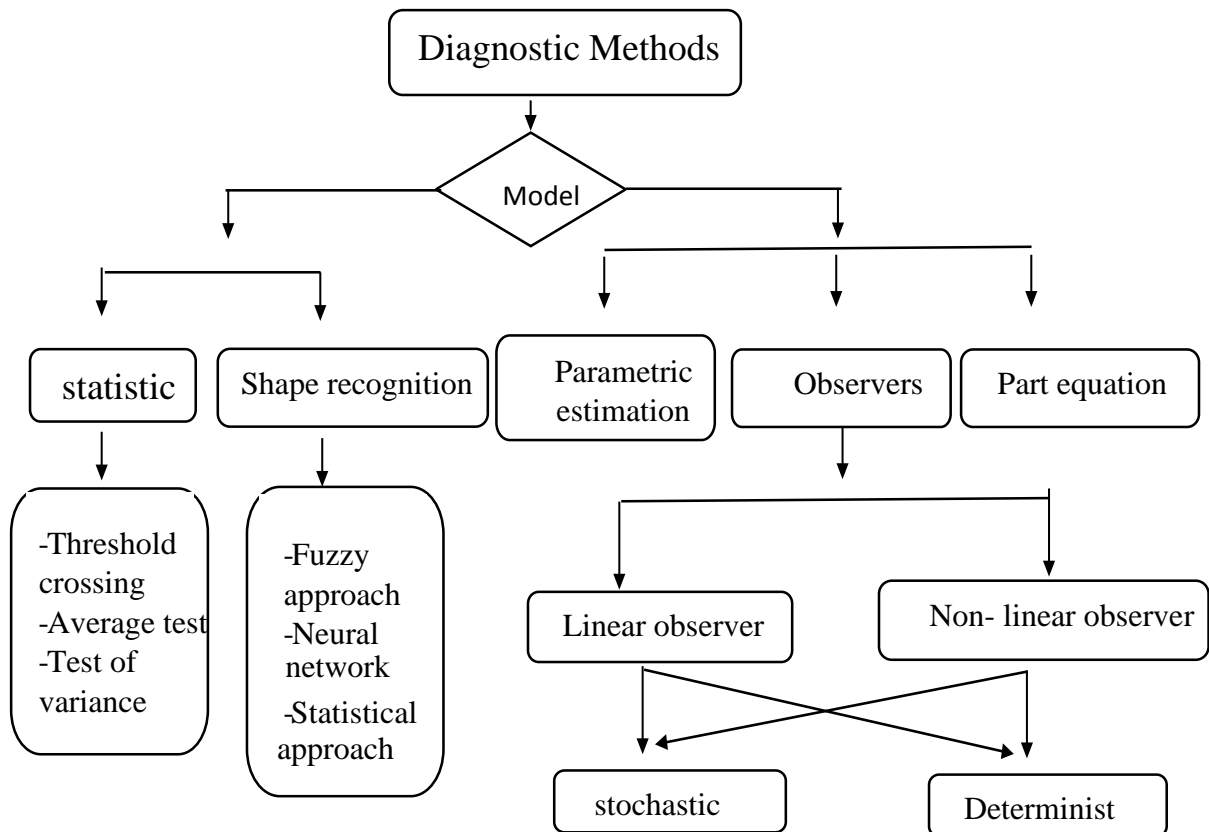


**Figure. I.10.** classification of diagnostic methods

### **I.10- Diagnostic techniques used to find problems with induction machines**

Various techniques are used to diagnose problems with induction machines. A method's dependability, speed of detection, and quantity of measured variables (required measurements) define it.

#### **1.10.1- Diagnostic methods based on external measurements:**

It is possible to diagnose the induction machine with the use of external data that was collected through various measurements. Among the non-invasive diagnostic methods are vibration analysis and spectrum analysis of the machine's absorbed stator currents. However, the imbalance in the power systems limits the ability to identify tiny amplitude problems in the winding of induction machines. Errors in the construction process and the non-ideal nature of the power supply are the causes of this imbalance.

#### **1.10.2- Analysis of the Park vector**

Using this method, a linear combination of the stator phase currents is the subject of investigation.  $i_{sa}(t)$ ,  $i_{sb}(t)$  and  $i_{sc}(t)$  The currents that were obtained  $i_{sd}(t)$  and  $i_{sq}(t)$  are provided by the subsequent

$$i_{sd} = \sqrt{\frac{2}{3}}i_{sa} - \frac{1}{\sqrt{6}}i_{sb} - \frac{1}{\sqrt{6}}i_{sc} \quad (1.1)$$

$$i_{sq} = \frac{1}{\sqrt{2}}i_{sb} - \frac{1}{\sqrt{2}}i_{sc} \quad (1.2)$$

In a perfect world,  $i_{sd}$  and  $i_{sq}$  is expressed as a function of time in the manner shown below:

$$i_{sq} = \frac{\sqrt{6}}{2}i \sin \left( \omega t - \frac{\pi}{2} \right) \quad (1.3)$$

$$i_{sd} = \frac{\sqrt{6}}{2}i \sin \left( \omega t - \frac{\pi}{2} \right) \quad (1.4)$$

$i$  : highest value of the supply current

$\omega$ : "stator pulsation."

The function's representation in the phase plane  $i_{sd} = f(i_{sq})$  allows for the acquisition of an indicator regarding the existence of imbalance. When everything is perfect—that is, when there are no faults or other imbalances and the power supply is sinusoidal—the curve that represents the function  $i_{sd} = f(i_{sq})$  is a round shape. This circle can be deformed to resemble an oval shape, which allows for the detection of imbalance caused by a problem or the power supply.

An experimental bench based on this method is provided in [15] for the purpose of stator defect identification. The flattening of the ellipse indicates the severity of the faults, while the elliptical shape derived in the phase plane gives information on their appearance.

The phase impacted by the defect is shown by the ellipse's main axis. The authors do not, however, explain how they distinguish between stator turns with intern-turn short faults  $s$  and stator supply voltage imbalances, which have similar consequences. Additionally, they don't say how to detect intern-turn intern-turn short-circuits that affect two phases.

Defect identification is carried out in [16] using the Park vector approach connected to neural network-based shape recognition. Shape identification is performed and an artificial neural network is developed in the case of a healthy machine as well as in specific fault scenarios. The writers only took into consideration a fairly small number of circumstances (open phase, unbalanced source, healthy motor). This approach would need retraining the neural network for every motor and the acquisition of data for every malfunction scenario in order to perform neural network learning.

### **I.10.3 Analysis of time-frequency and time-scale**

A technique for analysis appropriate for non-stationary signals is wavelet decomposition. It enables the information to be focused on coefficients that show the presence of a fault. In some cases, the stator current might be regarded as non-stationary. This kind of signal can be considered thanks to time-frequency modifications. The resultant image can be challenging to read, and the computation

time may be prohibitive. Wavelets are an effective tool for defect diagnosis in machines that operate at changing speeds because they may be utilized for localized analysis of signals in the time-frequency and time-scale domains.

#### **I.10.4 Analysis of stator currents**

New lines develop in the stator current spectrum, and some lines are emphasized, indicating that there are flaws in a specific area of the machine. An intriguing way to learn about the mechanical, electrical, and magnetic conditions of the machine is to analyze the frequency spectrum of the stator currents. It is among the most popular techniques that makes it possible to find a lot of flaws. Numerous methods for analyzing the signal to identify flaws are provided in the literature [17, 18].

#### **I.10.5 Analysis of instantaneous power**

Richer information is obtained from analyzing a phase's instantaneous power than from current analysis alone. Indeed, the power spectrum includes a component at the rotor failure frequency in addition to the fundamental component and the two side bands. This type of examination is more appropriate for identifying mechanical defects (such as damaged bearings). The same drawbacks that affect the approach involving spectral analysis of stator currents also affect this one. The ability to measure a single voltage and current is its primary benefit. The frequency spectrum is noisier.

#### **I.10.6 Spectral analysis of the stator current after power cut**

Stator turns intern-turn short-circuits are detected using this method in [18]. On a phase opening test, it is based. Cutting the stator supply voltages removes the source's impact, and the rotor currents cause the stator winding to become voltage-induced. The spectral analysis of line voltages forms the basis of the fault detection technique.

#### **I.10.7 Using symmetric components**

This technique for finding defects in the asynchronous machine is based on measuring the forward and reverse impedances, as well as the positive and negative sequence currents and voltages [19]. The asynchronous machine's impedances can be found via measurements of current and voltage. It creates an impedance value library for various rotation speeds. The supply voltages and currents can then be continuously measured in order to keep an eye on the asynchronous machine. It is possible to identify the existence of a degradation, such as intern-turn short-circuits of phase turns or intern-turn short-circuits between phases, by comparing the two sets of data.

This method's primary benefit is that constriction flaws don't affect the defect detecting system. Upon the formation of the parameter library, the monitoring process begins. Instrumentation is needed for this method to measure voltage, current, and speed. During the library formation phase, it is imperative to maintain a steady rotation speed and to keep the neutral current close to zero.

#### **I.10.8 Diagnostic methods with mathematical models**

Analytical or functional data about the system under observation can be used to perform fault diagnosis based on mathematical models [3,4,5,6,7,8,9,10,11,12,13, 14]. The system's mathematical model serves as the foundation for analytical redundancy techniques. They require comparing the changes in the quantities supplied by the model with the results derived from the process's measurements

(Figure. I.6). A group of signals known as residues hold the comparison's outcome. The latter's analysis enables the monitoring system's aberrant behavior to be recognized and understood.

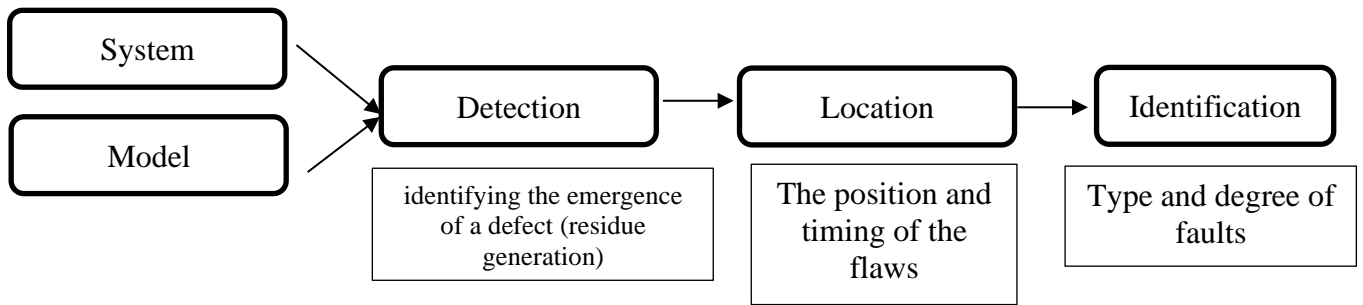


**Figure I.11** Process for identifying and isolating faults.

For analytical model-based diagnostics, three methods are employed:

- Approach to parametric estimation
- Parity equation procedure.
- Observer approach

Because it influences the monitoring system's quality, residue formation is a crucial part of the diagnostic process.

#### **I.10.9. Parametric estimation method**

The process of parameter estimation entails performance criterion optimization. Techniques for parametric estimating have undergone extensive research and testing [3]. On actual data, it is feasible to acquire trustworthy and realistic estimations thanks to output error approaches.

The process of determining the physical parameters (or structural parameters in the event that physical quantities are not accessible) included in the system's knowledge model is the foundation for fault detection and localization using parametric estimate. This mathematical model needs to be able to distinguish between operations that are defect-free and those that are not. When a defect results in a parametric variation, it becomes feasible to identify the existence of an imbalance in the machine by the estimation of the model variables [21]. A methodology for doing parametric estimation-based asynchronous machine diagnosis is described in [20]. A model specifically for diagnosis has been created, and a vector of parameters that need to be estimated has been specified.

The four traditional machine parameters are contained in the latter.  $(r_s, r_r, l_s, l_r)$  grew with variables connected to the faults taken into consideration  $(n_a, n_b, n_c)$

$$\theta = [r_s \ r_r \ l_s \ l_r \ n_a \ n_b \ n_c] \quad (1.5)$$

The diagnosis is subsequently made possible by identifying this vector of parameters using a parametric estimate technique. A criterion for composite minimization is created. It enables the

introduction of baseline information about the operating machine as well as data measured at the output that reveals the machine's current condition. The following are this approach's drawbacks:

the requirement to continuously introduce high-frequency excitation, which might have unfavorable effects like oscillations, for systems with variable speed drives.

The induction machine cannot be monitored in real time by using an offline reduction approach.

#### **I.10.10. induction machine diagnosis with parity equations**

This method's basic idea is to change the model's equations to produce specific links known as analytical redundancy relationships (ARR), which have the characteristic of only connecting known values [12, 13, 14]. One general difficulty of reducing variables in a system of algebraic differential equations is to obtain RRA offline. Projecting into the parity space is how the elimination is done in the linear case. Formal elimination techniques can be applied in the nonlinear situation.

[22] employed the parity space approach to identify asynchronous machine faults. Its nonlinear equations are described discretely using it. The model equations are rearranged to produce parity connections. Compute the partial derivatives of the residuals with respect to the model parameters in order to implement this approach. In terms of the parameters and state variables, these are non-linear. A group of residues that are susceptible to the five factors  $(r_s, l_s, r_r, l_r, M)$  is defined for the asynchronous machine. The residues are structured in order to make fault isolation easier. Applying this strategy to the asynchronous machine's nonlinear model is challenging. Furthermore, it is challenging to prove the discretized model's validity within the operating speed range.

#### **I.10.11-Using observers to diagnose the asynchronous machine**

Observers are dynamic systems that enable the state vector to be reconfigured. Both linear and nonlinear systems have benefited greatly from their widespread application. Using quantifiable signals from the system under observation, observers are used to rebuild the output vectors entirely or partially in order to discover faults. The creation of residues is made possible by the discrepancy between the reconstructed and actual outputs (**Figure I.7**). An observer for control and an observer for fault detection are not the same thing, though. The latter is done using the flawless system as a foundation. In fact, as long as there are no problems, some input signals that reflect the defects are unknown inputs that should remain equal to zero. They are not zero when a defect manifests. The observer then has to rapidly respond to this novel circumstance by pointing out any faults. The observer synthesis process needs to be done in a way that both detects errors and mitigates the impact of disruptions in order to produce a dependable detection system. To accomplish this goal, a nonlinear or linear decoupled observer with uncertain inputs was suggested. [6, 7,8,9,10,11] The primary strategy is to employ a state transition.  $z=T(x)$  ( $z=T(x)$  with  $T$  constant in the linear case ). to extract a portion of the state vector  $z$ , whose dynamics are separated from the unidentified inputs  $d$ . There are two stages that must be taken:

- creation of a disconnected state.
- Synthesis of observers and creation of residuals

A method for defect identification using linear observers and unknown inputs is provided in [26]. Fault are viewed as variations of the equivalent resistance (that of the Park model), which is the basis for the application of the Park model.

A collection of residues is created. It is not very practical to suppose that an identical defect would occur on all three phases at the same time as the fluctuation of the equivalent resistance does. Furthermore, this model does not account for the fluctuation in inductance caused by the influence of a stator turns intern-turn short-circuits failure.

The Park model associated with the stator or  $(\alpha, \beta)$  model of the induction machine is subjected to a Taylor series expansion in [22]. It enables the acquisition of a representation that considers changes in the parameters (resistance and inductance) surrounding an operational point. The nonlinear decoupling of defects and disturbances is achieved by a geometric approach, which is then followed by observer synthesis for defect detection. The model employed in this method is local, meaning it is only valid in the vicinity of an operating point; its exact validity is unknown. It can be challenging to discern between a variance resulting from an issue and one arising from the engine's regular operation.

[22] provides a technique for identifying and locating stator turn intern-turn short-circuits issues. It is predicated on using a sliding mode observer and appropriately characterizing the induction machine.

## **Conclusion**

Several diagnostic techniques based on analytical models were introduced in the earlier section of this chapter; the residual generation phase is crucial. Approaching a base of observers is one intriguing way to solve this issue. Real-time fault detection is made possible by the observer's concurrent operation with the monitored system. However, it is important to possess a suitable mathematical model of the observed system, wherein malfunctions and disruptions function as input signals. The induction machine modeling techniques, potential flaws, and detection strategies are covered in the second section. First, those that don't use mathematical models and are based on external measurements are shown. Next, a review is conducted on the use of the techniques mentioned in the first section in identifying asynchronous machine defects. It turns out that the diagnostic procedure's success greatly depends on the model that is used. In order to address this, we will spend the upcoming chapter creating new asynchronous machine models specifically for stator defects, or intern-turn intern-turn short-circuits in stator turns.

# **ChapterII**

## **Modeling Of Induction Machine**

## II.Introduction

The majority of faults that cause the induction machine to malfunction either in the closed or open loop is caused by turn intern-turn short-circuits faults in the stator phases.

In this section, we will introduce simplifying hypotheses to create a nonlinear model with variable coefficients and present the modeling of the induction machine without flaws for the synthesis of the control. The Park transformation, which is connected to the stator, is used to create a model that solely considers speed. Second, we use the methods described in [22,27] to model the induction machine in the presence of a stator turns intern-turn short-circuits defect for diagnostic reasons. We see that the model that is produced is multiplicative. Lastly, we demonstrate the induction machine's vector control with rotor flux orientation.

### II.1 Modeling of the healthy asynchronous machine:

Consider a squirrel cage machine having (3) identical windings symmetrical to the stator each of which is treated as a separate winding (Figure. 2.1.a) [7].

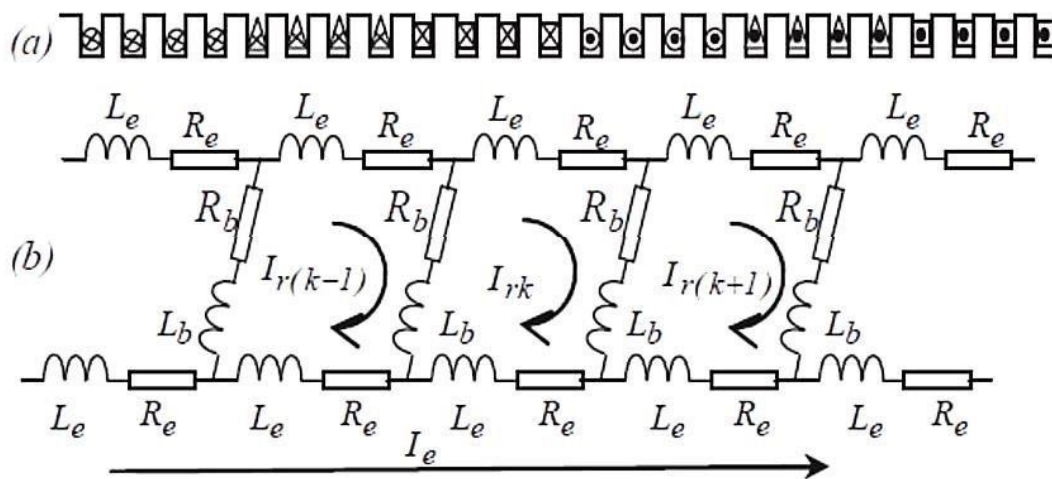


**Figure II.1** Structure of the stator (a) and rotor (b).

The rotor is considered as a mesh circuit, that is to say made up of a number (Nbr) of identical and equidistant bars short-circuited at both ends by two identical rings (Figure.2.1.b).

### II.2. Modeling Without Fault

A number of theories must be relied upon in order to develop relationships between the motor supply voltages and its currents. These include: flawless symmetry in the rotor and stator structure. integration of the cage into a intern-turn short-circuits winding that shares the rotor winding's phase count.

The distribution of each winding's magnetic fields is sinusoidal along the air gap.

Saturation is absent from the magnetic circuit.



## II.2.1 Magnetic representation

An additional three-phase winding on three rotor phases (a,b,c.) and one in relation to the other of 120° electric are represented by the three phase-shifted stator axes (a, b, and c) of the induction motor. In a vertical part of the machine, Figure 2.1 displays the electrical representation of the stator and rotor phases:

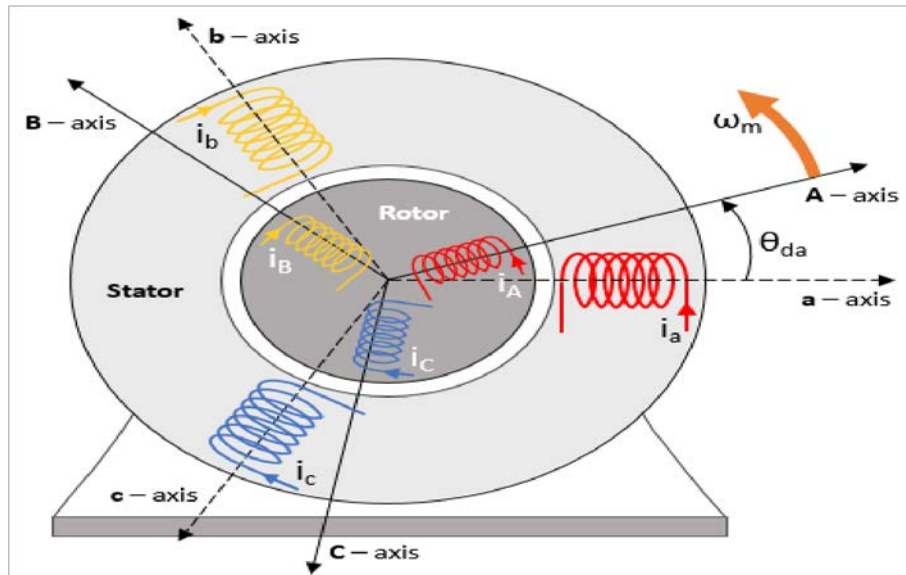


**Figure. II.1.** Model of a three-phase induction machine

A mesh consisting of a winding connected in series with an electrical resistance is a stator or rotor phase  $x$ . An electric current  $i_x$  of phase  $x$  flows through the entire area  $(a, b, c)$ . The induction machine electrical diagram is displayed in Figure 2.2.

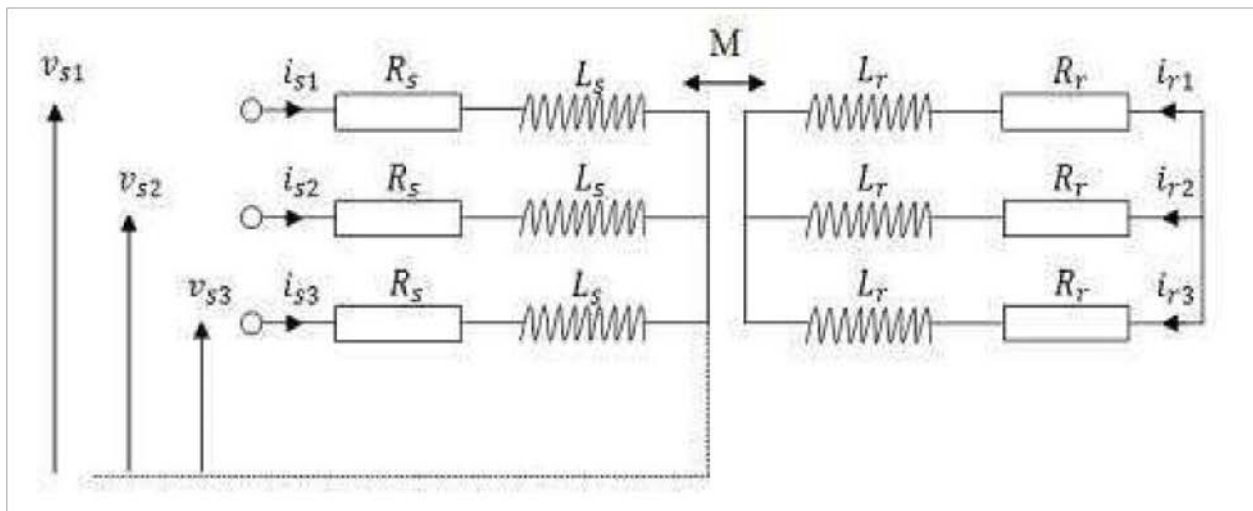


**Figure II.2** Representation of induction machine

We may write the following relationship on this mesh by using the Ohm-Faraday law:

$$U = RI + \frac{d\phi}{dt} \quad (2.1)$$

The voltage formulae are as follows for all stator phases:

$$\begin{bmatrix} u_{sa} \\ u_{sb} \\ u_{sc} \end{bmatrix} = \begin{bmatrix} R_s & 0 & 0 \\ 0 & R_s & 0 \\ 0 & 0 & R_s \end{bmatrix} \begin{bmatrix} i_{sa} \\ i_{sb} \\ i_{sc} \end{bmatrix} + \frac{d}{dt} \begin{bmatrix} \Phi_{sa} \\ \Phi_{sb} \\ \Phi_{sc} \end{bmatrix} \quad (2.2)$$

The following will be the matrix representation of equation (2.2):

$$[U_s] = [R_s] \cdot [I_s] + \frac{d}{dt} [\Phi_s] \quad (2.3)$$

Similarly, for every rotor phase that is short-circuited, we have:

$$\begin{bmatrix} u_{ra} \\ u_{rb} \\ u_{rc} \end{bmatrix} = \begin{bmatrix} R_r & 0 & 0 \\ 0 & R_r & 0 \\ 0 & 0 & R_r \end{bmatrix} \begin{bmatrix} i_{ra} \\ i_{rb} \\ i_{rc} \end{bmatrix} + \frac{d}{dt} \begin{bmatrix} \Phi_{ra} \\ \Phi_{rb} \\ \Phi_{rc} \end{bmatrix} = \begin{bmatrix} 0 \\ 0 \\ 0 \end{bmatrix} \quad (2.4)$$

The following is the matrix representation of equation (2.4):

$$[U_r] = [R_r] \cdot [I_r] + \frac{d}{dt} [\Phi_r] = [0] \quad (2.5)$$

With:

$$[I_s] = \begin{bmatrix} i_{sa} \\ i_{sb} \\ i_{sc} \end{bmatrix}, [I_r] = \begin{bmatrix} i_{ra} \\ i_{rb} \\ i_{rc} \end{bmatrix} \quad (2.6)$$

$$[U_s] = \begin{bmatrix} u_{sa} \\ u_{sb} \\ u_{sc} \end{bmatrix}, [U_r] = \begin{bmatrix} u_{ra} \\ u_{rb} \\ u_{rc} \end{bmatrix} \quad (2.7)$$

$$[\Phi_s] = \begin{bmatrix} \Phi_{sa} \\ \Phi_{sb} \\ \Phi_{sc} \end{bmatrix}, [\Phi_r] = \begin{bmatrix} \Phi_{ra} \\ \Phi_{rb} \\ \Phi_{rc} \end{bmatrix} \quad (2.8)$$

$[I_s]$ ,  $[U_s]$ ,  $[\Phi_s]$  stand for the phase fluxes, voltages, and stator currents.

$[I_r]$ ,  $[U_r]$ ,  $[\Phi_r]$  stand for the phase fluxes, voltages, and rotor currents.

$[R_s]$ ,  $[R_r]$  Represent the rotor and stator resistance matrices.

A coil's flux is determined by the current passing through it as well as the mutual inductances of the coils around it.

The following represents the stator fluxes:

$$[\Phi_s] = [L_s][I_s] + [M_{sr}][I_r] \quad (2.9)$$

The following represents the rotor fluxes:

$$[\Phi_r] = [L_r][I_r] + [M_{rs}][I_s] \quad (2.10)$$

It makes it possible to express the flows as a matrix:

$$\begin{bmatrix} \Phi_s \\ \Phi_r \end{bmatrix} = \begin{bmatrix} [L_s] & [M_{sr}] \\ [M_{rs}] & [L_r] \end{bmatrix} \begin{bmatrix} I_s \\ I_r \end{bmatrix} \quad (2.11)$$

With:

$$[L_s] = \begin{bmatrix} (l_{s\sigma} + M) & -\frac{1}{2}M & -\frac{1}{2}M \\ -\frac{1}{2}M & (l_{s\sigma} + M) & -\frac{1}{2}M \\ -\frac{1}{2}M & -\frac{1}{2}M & (l_{s\sigma} + M) \end{bmatrix} \quad (2.12)$$

$$[L_r] = \begin{bmatrix} (l_{r\sigma} + M) & -\frac{1}{2}M & -\frac{1}{2}M \\ -\frac{1}{2}M & (l_{r\sigma} + M) & -\frac{1}{2}M \\ -\frac{1}{2}M & -\frac{1}{2}M & (l_{r\sigma} + M) \end{bmatrix} \quad (2.13)$$

$$[M_{sr}] = [M_{rs}]^T = M \begin{bmatrix} \cos(\theta) & \cos(\theta + 2/3\pi) & \cos(\theta - 2/3\pi) \\ \cos(\theta - 2/3\pi) & \cos(\theta) & \cos(\theta + 2/3\pi) \\ \cos(\theta + 2/3\pi) & \cos(\theta - 2/3\pi) & \cos(\theta) \end{bmatrix} \quad (2.14)$$

With:

$[L_s]$ ,  $[L_r]$  represent the rotor and stator inductance matrices.

$[M_{sr}]$ ,  $[M_{rs}]$  represent the mutual inductance matrices between the rotor and stator.

Equations (2.3), (2.5), (2.9), and (2.10) illustrate how the induction machine operates.

## II.2.2 Representation of an electrical state:

Four (04) matrix equations are available to us:

$$\begin{cases} [U_s] = [R_s][I_s] + \frac{d}{dt}[\Phi_s] \\ [U_r] = [R_r][I_r] + \frac{d}{dt}[\Phi_r] = 0 \\ [\Phi_s] = [L_s][I_s] + [M_{sr}][I_r] \\ [\Phi_r] = [L_r][I_r] + [M_{rs}][I_s] \end{cases} \quad (2.15)$$

The stator currents were the main focus of the state variable selection.  $[I_s]$  and the rotor fluxes  $[\Phi_r]$ .

We can infer the following from equations (2.15)'s second and fourth:

$$\frac{d}{dt}[\Phi_r] = [R_r][L_r^{-1}][M_{rs}][I_s] - [R_r][L_r^{-1}][\Phi_r] \quad (2.16)$$

The following results from the third equation's derivation (2.15):

$$\frac{d}{dt}[\Phi_s] = \frac{d}{dt}([L_s][I_s] + [M_{sr}][L_r^{-1}]([\Phi_r] - [M_{rs}][I_s])) \quad (2.17)$$

$$\begin{aligned} \frac{d}{dt}[\Phi_s] &= \frac{d}{dt}[L_s][I_s] + [L_s]\frac{d}{dt}[I_s] + \frac{d}{dt}([M_{sr}][L_r^{-1}][\Phi_r] + [M_{sr}][L_r^{-1}]\frac{d}{dt}[\Phi_r] \\ &\quad - \frac{d}{dt}([M_{sr}][L_r^{-1}][M_{rs}][I_s]) - [M_{sr}][L_r^{-1}][M_{rs}]\frac{d}{dt}[I_s] \end{aligned} \quad (2.18)$$

Replacing  $\frac{d}{dt}[\Phi_r]$  in (2.18) By using equation (2.16) for its expression and plugging everything into the first equation of (2.15), we get:

$$\begin{aligned} &([L_s] - [M_{sr}][L_r^{-1}][M_{rs}])\frac{d}{dt}[I_s] = \\ &\left(-[R_s] - \frac{d}{dt}([L_s] - [M_{sr}][L_r^{-1}][M_{rs}]) - ([M_{sr}][L_r^{-1}][R_r][L_r^{-1}][M_{rs}])\right)[I_s] \\ &+ \left([M_{sr}][L_r^{-1}][R_r][L_r^{-1}] - \frac{d}{dt}([M_{sr}][L_r^{-1}])\right)[\Phi_r] + [U_s] \end{aligned} \quad (2.19)$$

It is possible to rewrite (2.19) as follows:

$$\frac{d}{dt} [I_s] = [\alpha_1^{-1}]([\alpha_2][I_s] + [\alpha_3][\Phi_r] + [U_s]) \quad (2.20)$$

With:

$$[\alpha_1] = [L_s] - [M_{sr}][L_r^{-1}][M_{rs}] \quad (2.21)$$

$$[\alpha_2] = -[R_s] - \frac{d}{dt}([L_s] - [M_{sr}][L_r^{-1}][M_{rs}]) - ([M_{sr}][L_r^{-1}][R_r][L_r^{-1}][M_{rs}]) \quad (2.22)$$

$$[\alpha_3] = ([M_{sr}][L_r^{-1}][R_r][L_r^{-1}]) - \frac{d}{dt}([M_{sr}][L_r^{-1}]) \quad (2.23)$$

Equations (2.16) and (2.20), which represent the electromagnetic part's equations, allow us to reformulate the system as an equation of state with variable coefficients.

$$\dot{x}(t) = A(\omega, t)x(t) + B(\omega, t)u(t) \quad (2.24)$$

Depending on the state variables selected:

$$\begin{cases} \frac{d}{dt} [I_s] = [A_{11}][I_s] + [A_{12}][\Phi_r] + [B_1][U_s] \\ \frac{d}{dt} [\Phi_r] = [A_{21}][I_s] + [A_{22}][\Phi_r] \end{cases} \quad (2.25)$$

Or:

$$\frac{d}{dt} \begin{bmatrix} I_s \\ \Phi_r \end{bmatrix} = \begin{bmatrix} A_{11} & A_{12} \\ A_{21} & A_{22} \end{bmatrix} \begin{bmatrix} I_s \\ \Phi_r \end{bmatrix} + \begin{bmatrix} B_1 \\ 0 \end{bmatrix} [U_s] \quad (2.26)$$

With:

$$\begin{cases} [A_{11}] = [\alpha_1^{-1}][\alpha_2] \\ [A_{12}] = [\alpha_1^{-1}][\alpha_3] \\ [A_{21}] = [R_r][L_r^{-1}][M_{rs}] \\ [A_{22}] = -[R_r][L_r^{-1}] \\ [B_1] = [\alpha_1^{-1}] \end{cases} \quad (2.27)$$

### II.2.3. Application of the Park transformation

We choose the Park transformation because the mathematical model of the induction machine in the three-phase frame is more intricate and non-linear. Physically, it may be explained by converting a three-phase system that is in balance into a two-phase system that matches the original machine's windings. These windings are equal from an electrical and magnetic standpoint and are organized in the plane (d,q) [27],[28].

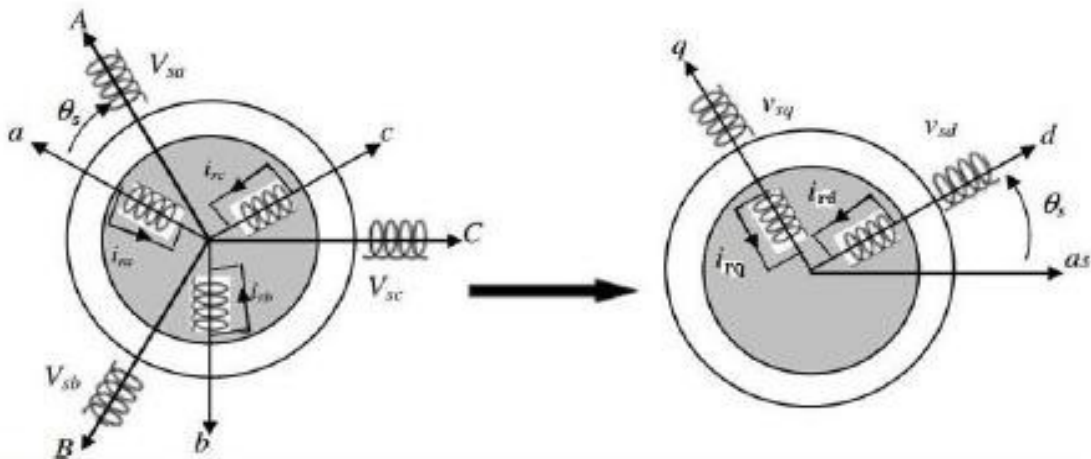


Figure 2.3: Park Transform illustration

The matrix  $P(\theta)$ , where  $\theta$  is the angle between the three-phase frame and the Park frame, guarantees this transformation:

$$P(\theta) = \sqrt{\frac{2}{3}} \begin{bmatrix} \cos \theta_s & \cos \left( \theta_s - \frac{2\pi}{3} \right) & \cos \left( \theta_s - \frac{4\pi}{3} \right) \\ -\sin(\theta_s) & -\sin \left( \theta_s - \frac{2\pi}{3} \right) & -\sin \left( \theta_s - \frac{4\pi}{3} \right) \\ \frac{1}{\sqrt{2}} & \frac{1}{\sqrt{2}} & \frac{1}{\sqrt{2}} \end{bmatrix} \quad (2.28)$$

The existence of the  $P(\theta)$  inverse matrix is crucial for the reconstitution of the variables in the ABC, where it is clear which is equal to its transposed and is expressed as follows:

$$[P(\theta)]^{-1} = [P(\theta)]^T \quad (2.29)$$

The Park frame calculates a variable X from the three-phase frame using the following relationship:

$$[X_p] = [P][X_{abc}] \quad (2.30)$$

From where:

$$[X_{abc}] = [P]^{-1}[X_p] = [P]^T[X_p] \quad (2.31)$$

Therefore, the state variables are as follows:

$$[I_{sdqo}] = [P_s][I_{sabc}] \quad (2.32)$$

$$[\Phi_{rdqo}] = [P_r][\Phi_{rabc}] \quad (2.33)$$

Or

$[P_s(\theta)]$  : Transformation de Park applied to the stator .

$[P_r(\theta)]$  : Transformation de Park applied to the rotor.

$$\begin{cases} \frac{d}{dt} [I_{sdqo}] = [P_s] \left( [A_{11}] [P_s^{-1}] - \frac{d}{dt} [P_s^{-1}] \right) [I_{sdqo}] + [P_s] [A_{12}] [P_r^{-1}] [\Phi_{rdqo}] + [P_s] [B_1] [P_s^{-1}] [U_s] \\ \frac{d}{dt} [\Phi_{rdqo}] = [P_r] [A_{21}] [P_s^{-1}] [I_{sdqo}] + [P_r] \left( [A_{22}] [P_r^{-1}] - \frac{d}{dt} [P_r^{-1}] \right) [\Phi_{rdqo}] \end{cases} \quad (2.34)$$

#### II.2.4 The machine's model in the frame connected to the stator field

Within a context connected to the stator field, we have ( $\theta_s = 0, \theta_r = \theta$ ) and the equation (2.34) model is transformed into:

$$\frac{d}{dt} \begin{bmatrix} I_{sdqo} \\ \Phi_{rdqo} \end{bmatrix} = \begin{bmatrix} A_{11p} & A_{12p} \\ A_{21p} & A_{22p} \end{bmatrix} \begin{bmatrix} I_{sdqo} \\ \Phi_{rdqo} \end{bmatrix} + \begin{bmatrix} B_{1p} \\ 0 \end{bmatrix} [U_s] \quad (2.35)$$

With:

$$[A_{11p}] = \begin{bmatrix} \alpha_1 & 0 & 0 \\ 0 & \alpha_1 & 0 \\ 0 & 0 & -R_s/L_s \end{bmatrix} \quad (2.36)$$

$$[A_{12p}] = \begin{bmatrix} \alpha_2 & \alpha_3 \omega & 0 \\ -\alpha_3 \omega & \alpha_2 & 0 \\ 0 & 0 & 0 \end{bmatrix} \quad (2.37)$$

$$[A_{21p}] = \begin{bmatrix} \alpha_4 & 0 & 0 \\ 0 & \alpha_4 & 0 \\ 0 & 0 & 0 \end{bmatrix} \quad (2.38)$$

$$[A_{22p}] = \begin{bmatrix} \alpha_5 & -\omega & 0 \\ \omega & \alpha_5 & 0 \\ 0 & 0 & -R_r/L_r \end{bmatrix} \quad (2.39)$$

$$[B_{1p}] = \begin{bmatrix} b_1 & 0 & 0 \\ 0 & b_1 & 0 \\ 0 & 0 & 1/L_s \end{bmatrix} \quad (2.40)$$

Appendix A contains the coefficients  $\alpha_i$  and  $b_1$ .

Appendix A has the induction machine model that is connected to the rotating field; this model is utilized to build the vector control with the rotor flux orientation.

### II.2.5 The Mechanical equation

When we apply the rotor to the fundamental law of mechanics, we get:

$$J \frac{d}{dt} \Omega = T_e - f_v \Omega - T_l \quad (2.41)$$

With:

$$\omega = 2\Omega \quad (2.42)$$

With:

$J, f_v, T_l, \Omega$  designate the rotor's moment of inertia, load torque, coefficient of viscous friction, and mechanical speed, in that order. The interaction of two fields—the rotor field from induced currents in the rotor and the stator field from the power supply's electromagnetic field—produces the electromagnetic torque. It is articulated by:

$$T_e = \frac{\partial W}{\partial \theta} = \frac{1}{2} [I]^T \frac{\partial}{\partial \theta} (L(\theta)) [I] \quad (2.43)$$

With:

$$[I] = \begin{bmatrix} I_s \\ I_r \end{bmatrix}, \frac{\partial}{\partial \theta} L(\theta) = \begin{bmatrix} 0 & \frac{\partial}{\partial \theta} M_{sr} \\ \frac{\partial}{\partial \theta} M_{rs} & 0 \end{bmatrix} \quad (2.44)$$

$p$ : The quantity of pole pairs.

Although it is simpler than the three-phase model, the induction machine model without flaws in the Park frame exhibits symmetry in these matrices and is nevertheless non-linear since the coefficients of its state matrix depend on the mechanical speed.

### II.3. Modeling With Fault

One or more stator phases experiencing a intern-turn intern-turn short-circuits is the stator issue under investigation [22, 27].

Think about the following terms:  $n_{cca}, n_{ccb}, n_{ccc}$  indicating the total number of turns in each phase, as well as the number of short-circuited turns.  $n_s$ .

Taking  $n_a, n_b, n_c$  the ratio of the total number of turns to the number of intern-turn intern-turn short-circuits turns with

$$n_a = \frac{n_{cca}}{n_s}, n_b = \frac{n_{ccb}}{n_s}, n_c = \frac{n_{ccc}}{n_s} \quad (2.46)$$

The turning ratios that are still in use can then be used as follows:

$$f_a = 1 - n_a, f_b = 1 - n_b, f_c = 1 - n_c \quad (2.47)$$

## II.1 Electrical equations represented with faults

$$[R_s] = rs \begin{bmatrix} f_a & 0 & 0 \\ 0 & f_b & 0 \\ 0 & 0 & f_c \end{bmatrix} \quad (2.48)$$

The mutual and internal inductance matrix of the stator is as follows:

$$[M_{ss}] = M \begin{bmatrix} f_a^2 & -\frac{1}{2}f_a f_b & -\frac{1}{2}f_a f_c \\ -\frac{1}{2}f_a f_b & f_b^2 & -\frac{1}{2}f_b f_c \\ -\frac{1}{2}f_a f_c & -\frac{1}{2}f_b f_c & f_c^2 \end{bmatrix} \quad (2.49)$$

The following represents the stator leakage inductance matrix:

$$[L_{s\sigma}] = l_{s\sigma} \begin{bmatrix} f_a^2 & 0 & 0 \\ 0 & f_b^2 & 0 \\ 0 & 0 & f_c^2 \end{bmatrix} \quad (2.50)$$

The following gives the stator inductance matrix:

$$[L_s] = [L_{s\sigma}] + [M_{ss}] \quad (2.51)$$

From where:

$$[L_s] = \begin{bmatrix} (l_{s\sigma} + M)f_a^2 & -\frac{1}{2}f_a f_b M & -\frac{1}{2}f_a f_c M \\ -\frac{1}{2}f_a f_b M & (l_{s\sigma} + M)f_b^2 & -\frac{1}{2}f_b f_c M \\ -\frac{1}{2}f_a f_c M & -\frac{1}{2}f_b f_c M & (l_{s\sigma} + M)f_c^2 \end{bmatrix} \quad (2.52)$$

The following represents the mutual inductance matrices between the rotor and stator:

$$[M_{sr}] = M \begin{bmatrix} f_a \cos(\theta) & f_a \cos\left(\theta + \frac{2\pi}{3}\right) & f_a \cos\left(\theta - \frac{2\pi}{3}\right) \\ f_b \cos\left(\theta - \frac{2\pi}{3}\right) & f_b \cos(\theta) & f_b \cos\left(\theta + \frac{2\pi}{3}\right) \\ f_c \cos\left(\theta + \frac{2\pi}{3}\right) & f_c \cos\left(\theta - \frac{2\pi}{3}\right) & f_c \cos(\theta) \end{bmatrix} \quad (2.53)$$

$$[M_{rs}] = [M_{sr}]^T \quad (2.54)$$

Because of the addition of turns ratios corresponding to each stator phase in the stator resistance and inductance matrices, the stator-rotor mutual inductance matrices, and the rotor-stator, the idea of symmetry observed in the machine's healthy model is no longer verified.

There is no modification to the rotor resistance and inductance matrices.

The induction machine's stator and rotor voltage equations are provided by:

$$[U_s] = [R_s][I_s] + \frac{d}{dt}[\Phi_s] \quad (2.55)$$

$$[U_r] = [R_r][I_r] + \frac{d}{dt}[\Phi_r] = 0 \quad (2.56)$$

The following are the flow equations:

$$[\Phi_s] = [L_s][I_s] + [M_{sr}][I_r] \quad (2.57)$$

$$[\Phi_r] = [M_{rs}][I_s] + [L_r][I_r] \quad (2.58)$$

The mechanical equation:

$$J \frac{d}{dt} \Omega = T_e - f_v \Omega - T_l \quad (2.59)$$

Due to the asymmetric matrices in this system, the Park transformation cannot be employed to resolve it. Consequently, a different transformation  $T$  is applied to the rotor quantities [36], which results in a projection of the rotor quantities onto the stator reference, which can be expressed as follows:

$$[T] = \frac{2}{3} \begin{bmatrix} \cos(\theta) + \frac{1}{2} & \cos\left(\theta + \frac{2\pi}{3}\right) + \frac{1}{2} & \cos\left(\theta - \frac{2\pi}{3}\right) + \frac{1}{2} \\ \cos\left(\theta - \frac{2\pi}{3}\right) + \frac{1}{2} & \cos(\theta) + \frac{1}{2} & \cos\left(\theta + \frac{2\pi}{3}\right) + \frac{1}{2} \\ \cos\left(\theta + \frac{2\pi}{3}\right) + \frac{1}{2} & \cos\left(\theta - \frac{2\pi}{3}\right) + \frac{1}{2} & \cos(\theta) + \frac{1}{2} \end{bmatrix} \quad (2.60)$$

The rotor currents and fluxes are subjected to this change in the following ways:

$$[I_r] = [T]^{-1}[I_r^*] \quad (2.61)$$

$$[\Phi_r] = [T]^{-1}[\Phi_r^*] \quad (2.62)$$

The rotor currents and fluxes are subjected to this change in the following ways:

$$[R_r][I_r^*] + [T] \frac{d}{dt} [T]^{-1}[\Phi_r^*] + \frac{d}{dt} [\Phi_r^*] = 0 \quad (2.63)$$

The two equations (2.57) and (2.58) become:

$$[\Phi_s] = [L_s][I_s] + [M_{sr}][T]^{-1}[I_r^*] \quad (2.64)$$

$$[\Phi_r^*] = [T][M_{rs}][I_s] + [T][L_r][T]^{-1}[I_r^*] \quad (2.65)$$

As a result, the electrical equation system becomes:

$$\begin{cases} [U_s] = [R_s][I_s] + \frac{d}{dt} [\Phi_s] \\ [R_r][I_r^*] + [T] \frac{d}{dt} [T]^{-1}[\Phi_r^*] + \frac{d}{dt} [\Phi_r^*] = 0 \\ [\Phi_s] = [L_s][I_s] + [M_{sr}^*][I_r^*] \\ [\Phi_r^*] = [M_{rs}^*][I_s] + [L_r^*][I_r^*] \end{cases} \quad (2.66)$$

With:

$$[M_{sr}^*] = [M_{sr}][T]^{-1} \quad (2.67)$$

$$[M_{rs}^*] = [T][M_{rs}] \quad (2.68)$$

$$[L_r^*] = [T][L_r][T]^{-1} \quad (2.69)$$

The mechanical formula remains unchanged.

Regarding the operational machine, we have selected the mechanical speed, rotor fluxes, and stator currents as state variables. Using the system's fourth equation (2.66), we obtain:

$$[I_r^*] = [L_r^*]^{-1}([\Phi_r^*] - [M_{rs}^*][I_s]) \quad (2.70)$$

The second equation in (2.66) is modified by adding (2.70):

$$\frac{d}{dt} [\Phi_r^*] = [R_r][L_r^*]^{-1}[M_{rs}^*][I_s] - \left([R_r][L_r^*]^{-1} + [T] \frac{d}{dt} [T]^{-1}\right) [\Phi_r^*] \quad (2.71)$$

$$\frac{d}{dt} [I_r^*] = \frac{d}{dt} ([L_r^*]^{-1})[\Phi_r^*] + [L_r^*]^{-1} \frac{d}{dt} [\Phi_r^*] - \frac{d}{dt} ([L_r^*]^{-1}[M_{rs}^*])[I_s] - [L_r^*]^{-1}[M_{rs}^*] \frac{d}{dt} [I_s] \quad (2.72)$$

$$\frac{d}{dt} [\Phi_s] = \frac{d}{dt} [L_s][I_s] + [L_s] \frac{d}{dt} [I_s] + \frac{d}{dt} [M_{sr}^*][I_r^*] + [M_{sr}^*] \frac{d}{dt} [I_r^*] \quad (2.73)$$



Replacing  $\frac{d}{dt}[I_r^*]$  and  $[I_r^*]$  By using their respective expressions of equations (2.72) and (2.70) in (2.73), we can determine the resultant in the first equation of (2.66), which is as follows:

$$[U_s] = \alpha_5[I_s] + \alpha_7 \frac{d}{dt}[I_s] + \alpha_6[\Phi_r^*] \quad (2.74)$$

With:

$$\alpha_5 = [R_s] - \left(\frac{d}{dt}[M_{sr}^*]\right)[L_r^*]^{-1}[M_{rs}^*] - [M_{sr}^*] \left(\frac{d}{dt}[L_r^*]^{-1}[M_{rs}^*]\right) + [M_{sr}^*][L_r^*]^{-1}[R_r][L_r^*]^{-1}[M_{rs}^*] \quad (2.75)$$

$$\alpha_6 = \left(\frac{d}{dt}[M_{sr}^*]\right)[L_r^*]^{-1} - [M_{sr}^*][L_r^*]^{-1} \left([R_r][L_r^*]^{-1} + [T] \frac{d}{dt}[T]^{-1}\right) \quad (2.76)$$

$$\alpha_7 = [L_s] - [M_{sr}^*][L_r^*]^{-1}[M_{rs}^*] \quad (2.77)$$

Lastly, this is the electrical model:

$$A_{m11} = -\alpha_7^{-1}\alpha_5 \quad (2.78)$$

$$A_{m12} = -\alpha_7^{-1}\alpha_6 \quad (2.79)$$

$$B_{m11} = \alpha_7^{-1} \quad (2.80)$$

$$A_{m21} = [R_r][L_r^*]^{-1}[M_{rs}^*] \quad (2.81)$$

$$A_{m22} = -\left([R_r][L_r^*]^{-1} + [T] \frac{d}{dt}[T]^{-1}\right) \quad (2.82)$$

For the mechanical equation  $T_e$  becomes :

$$T_e = \left(\frac{\sqrt{3}M}{3M+2L_r}\right) (f_b I_{sb} (-\Phi_{rc}^* + \Phi_{ra}^*) + f_c I_{sc} (-\Phi_{ra}^* + \Phi_{rb}^*) + f_a I_{sa} (-\Phi_{rb}^* + \Phi_{rc}^*)) \quad (2.83)$$

### II.3.1 Multiplicative representation of the model

The resulting multiplicative induction machine model will be represented by the following seven state variables:

Three stator currents.

Three flows of rotors.

Speed of a machine.

Consequently, the state vector is:

$$[X] = \begin{bmatrix} x_1 \\ x_2 \\ x_3 \\ x_4 \\ x_5 \\ x_6 \\ x_7 \end{bmatrix} = \begin{bmatrix} I_{sa} \\ I_{sb} \\ I_{sc} \\ \Phi_{ra}^* \\ \Phi_{rb}^* \\ \Phi_{rc}^* \\ \Omega \end{bmatrix} \quad (2.84)$$

We were able to build the following matrices thanks to the mathematical evolution of the state matrices of the model previously mentioned in (2.78).

$$[A_{m11}] = \begin{bmatrix} \frac{a_1}{f_a} + a_2 & \frac{(a_3+a_4fb)}{f_a} & \frac{(a_3+a_4fc)}{f_a} \\ \frac{(a_3+a_4fa)}{f_b} & \frac{a_1}{f_b} + a_2 & \frac{(a_3+a_4fc)}{f_b} \\ \frac{(a_3+a_4fa)}{f_c} & \frac{(a_3+a_4fb)}{f_c} & \frac{a_1}{f_c} + a_2 \end{bmatrix} \quad (2.85)$$

$$[A_{m12}] = \begin{bmatrix} \frac{2a_5}{f_a} & \frac{(-a_5+a_6\omega)}{f_a} & \frac{(-a_5-a_6\omega)}{f_a} \\ \frac{(-a_5-a_6\omega)}{f_b} & \frac{2a_5}{f_b} & \frac{(-a_5+a_6\omega)}{f_b} \\ \frac{(-a_5+a_6\omega)}{f_c} & \frac{(-a_5-a_6\omega)}{f_c} & \frac{2a_5}{f_c} \end{bmatrix} \quad (2.86)$$

$$[A_{m22}] = \begin{bmatrix} a_8 & a_9 + \frac{\sqrt{3}}{3}\omega & a_9 - \frac{\sqrt{3}}{3}\omega \\ a_9 - \frac{\sqrt{3}}{3}\omega & a_8 & a_9 + \frac{\sqrt{3}}{3}\omega \\ a_9 + \frac{\sqrt{3}}{3}\omega & a_9 - \frac{\sqrt{3}}{3}\omega & a_8 \end{bmatrix} \quad (2.87)$$

$$[B_{m11}] = \begin{bmatrix} \frac{b_1}{f_a^2} & \frac{b_2}{fafb} & \frac{b_2}{fafc} \\ \frac{b_2}{fafb} & \frac{b_1}{f_b^2} & \frac{b_2}{fbfc} \\ \frac{b_2}{fafc} & \frac{b_2}{fbfc} & \frac{b_1}{f_c^2} \end{bmatrix} \quad (2.88)$$

The coefficients  $a_i$  et  $b_i$  are given in Appendix A:

This model contains faults in the form of turns ratios as a function, which are represented by  $f_a, f_b, f_c$ .

### II.3.2 Application of the Park transformation linked to the stator

The stator frame contains representations for all state variables, currents, and flows. The transformation T, which was applied to the rotor sizes, is used to project the flows onto the stator frame.

The passage matrix  $P_s(\Psi)$ , connected to the stator ensures the Park transition. ( $\Psi = 0$ ) The source of this matrix is:

$$P_s(\Psi)l_{\Psi=0} = \sqrt{\frac{2}{3}} \begin{bmatrix} 1 & \frac{-1}{2} & \frac{-1}{2} \\ 0 & \frac{\sqrt{3}}{2} & \frac{\sqrt{3}}{2} \\ \frac{1}{\sqrt{2}} & \frac{1}{\sqrt{2}} & \frac{1}{\sqrt{2}} \end{bmatrix} \quad (2.89)$$

Given that this matrix is unitary, its transpose yields its inverse.

$$[P(0)]^{-1} = [P(0)]^T \quad (2.90)$$

After the multiplicative model is transformed in this way, we get:

$$\begin{cases} \frac{d}{dt} [I_{sdqo}] = [P_s] \left( [A_{m11}][P_s^{-1}] - \frac{d}{dt} [P_s^{-1}] \right) [I_{sdqo}] + [P_s][A_{m12}][P_s^{-1}][\Phi_{rdqo}] + [P_s][B_{m11}][P_s^{-1}][U_s] \\ \frac{d}{dt} [\Phi_{sdqo}] = [P_s][A_{m21}][P_s^{-1}][I_{sdqo}] + [P_s] \left( [A_{m22}][P_s^{-1}] - \frac{d}{dt} [P_s^{-1}] \right) [\Phi_{rdqo}] \end{cases} \quad (2.91)$$

The electromagnetic component of the multiplicative model in the Park reference frame is obtained by doing the required computations, and the model will be:

$$\begin{cases} \frac{d}{dt}[I_{sdqo}] = [A_{m11p}][I_{sdqo}] + [A_{m12p}][\Phi_{rdqo}] + [B_{m11p}][U_s] \\ \frac{d}{dt}[\Phi_{rdqo}] = [A_{m21p}][I_{sdqo}] + [A_{m22p}][\Phi_{rdqo}] \end{cases} \quad (2.92)$$

Or:

$$[A_{m11p}] = [P_s] \left( [A_{m11}][P_s^{-1}] - \frac{d}{dt}[P_s^{-1}] \right) \quad (2.93)$$

$$[A_{m12p}] = [P_s][A_{m12}][P_s^{-1}] \quad (2.94)$$

$$[A_{m21p}] = [P_s][A_{m21}][P_s^{-1}] \quad (2.95)$$

$$[A_{m22p}] = [P_s] \left( [A_{m22}][P_s^{-1}] - \frac{d}{dt}[P_s^{-1}] \right) \quad (2.96)$$

$$[B_{m11p}] = [P_s][B_{m11}][P_s^{-1}] \quad (2.97)$$

The electromagnetic torque formula looks like this:

$$\begin{aligned} T_e = cp \left( -\sqrt{2}f_a \left( \frac{\sqrt{6}}{3}i_{sd} + \frac{\sqrt{3}}{3}i_{so} \right) \Phi_{rq} - f_b \left( -\frac{\sqrt{6}}{6}i_{sd} + \frac{\sqrt{2}}{2}i_{sq} + \frac{\sqrt{3}}{3}i_{so} \right) \left( \frac{\sqrt{6}}{2}\Phi_{rd} + \frac{\sqrt{2}}{2}\Phi_{rq} \right) \right. \\ \left. + f_c i_{sc} \left( -\frac{\sqrt{6}}{2}\Phi_{rd} + \frac{\sqrt{2}}{2}\Phi_{rq} \right) \right) \end{aligned} \quad (2.98)$$

## Conclusion

in this chapter the modeling of the asynchronous machine is carried out in two cases, with and without intern-turn short-circuits faults of stator turns. In the case of absence of faults the model obtained presents a symmetry it is used for the synthesis of the speed estimator in the case of the machine healthy.

Two models are obtained in the case of the presence of defects, three-phase multiplicative and two-phase multiplicative in Park. These two models are unbalanced. The defects are reflected by the quantities of turns still in function. The latter will be used for the detection of turn intern-turn short faults s. A Brief Introduction to Orientation Vector Control of rotor flux was presented to study the different cases of operation of the asynchronous machine.

# **Chapitre III**

## **Fault Detection Using d-q Analysis**

### III.Introduction

In this chapter, we delve into fault detection using d-q analysis (Park transformation) and the simulation of induction machines both with and without faults, accompanied by the analysis of results. The utilization of d-q analysis, through Park transformation, provides a powerful technique for studying machine behavior under faulty conditions. By transforming the three-phase quantities into a two-axis reference frame aligned with the rotor flux, fault detection becomes more intuitive and manageable.

Through simulation, we explore the performance of induction machines in healthy operating conditions as well as when subjected to faults such as stator winding short-circuits. This approach allows for a comprehensive understanding of how faults manifest in the machine's behavior and how they can be detected and diagnosed using advanced analytical methods.

The results obtained from these simulations provide valuable insights into the effectiveness of fault detection strategies based on d-q analysis, highlighting the benefits of such approaches in practical machine monitoring and maintenance. By the end of this chapter, readers will gain a deeper appreciation of fault detection techniques and their application in ensuring the reliability and efficiency of induction machine operations.

#### III.1- Simulation of an induction machine without faults

We begin with a balanced network-powered simulation of an induction machine in an error-free scenario. Next, a voltage imbalance in the supply is introduced. Additionally, the rotor speed and flux estimation are done.

##### III.1.2 -Balanced three-phase power supply

The fault-free induction machine model found in equation (2.35) is the one that was examined in this instance. Initially, a balanced three-phase network powers the machine.

Equation (4.1) provides the three-phase voltage that powers the induction machine in a balanced manner.

$$U_s = \begin{bmatrix} 220\sqrt{2} \sin(2\pi ft) \\ 220\sqrt{2} \sin\left(2\pi ft + \frac{2\pi}{3}\right) \\ 220\sqrt{2} \sin\left(2\pi ft - \frac{2\pi}{3}\right) \end{bmatrix} \quad (4.1)$$

The results of the without any flaws induction machine simulation are shown in figures (3.1, 3.2, 3.3, 3.5, 3.6, 3.7. ) Stator currents, rotor flux, mechanical speed, and electromechanical torque are the factors that are mentioned.

Assuming that the machine is powered by the voltage specified in (3.1), we can apply a 5Nm load torque at time 0.5s. The supply voltages, stator currents, rotor flux, electromechanical torque, and rotor rotation speed are all depicted in the following figures.

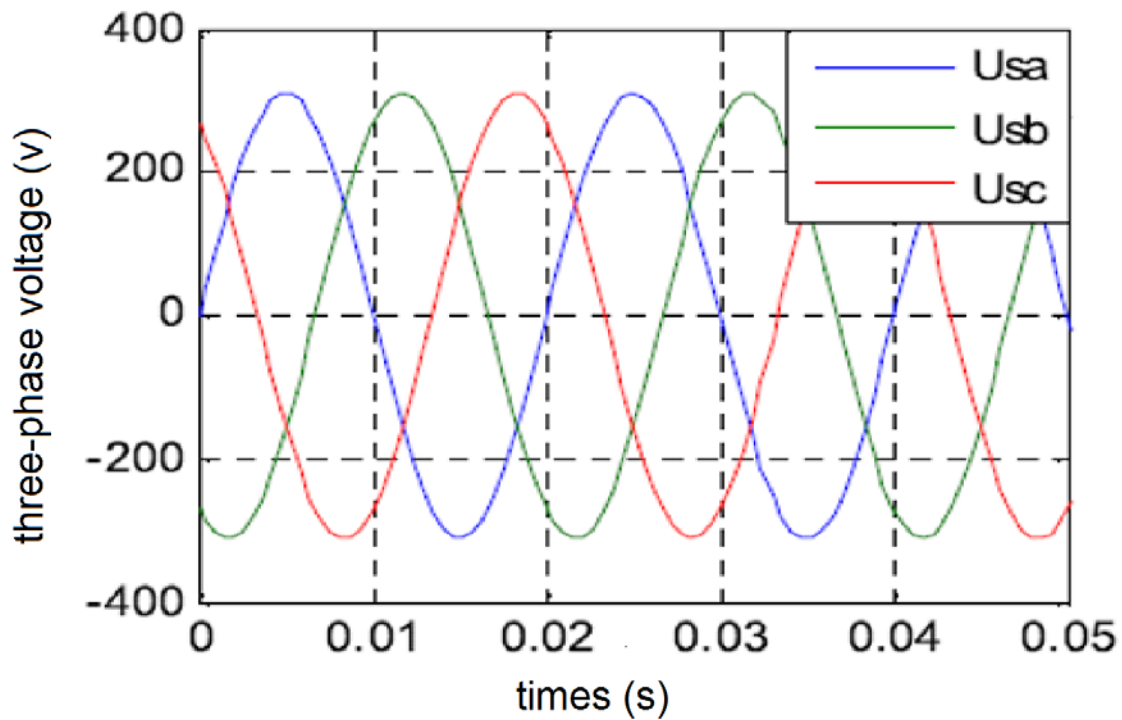


**Figure III.1:** The supply voltage in the three-phase

The progression of the supply voltages is depicted in figures (a) and (b), respectively, in the three-phase and two-phase marks. For the three-phase frame, the voltages are sinusoidally phase-shifted by  $\frac{2\pi}{3}$ , and for the two-phase Park frame, they are phase-shifted in quadrature.

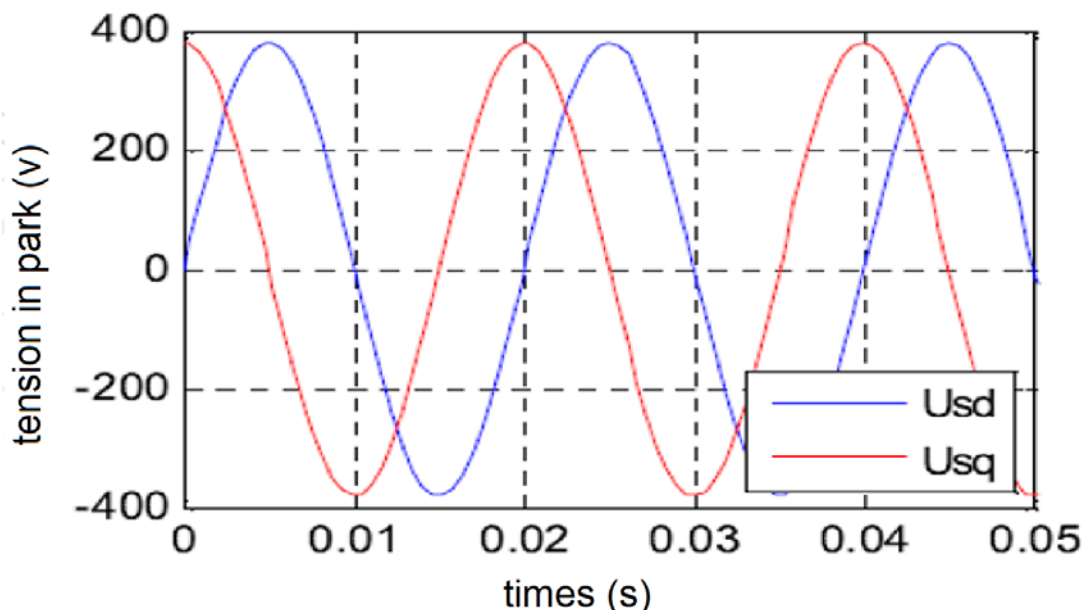


**Figure III.2:** The supply voltage in two-phase

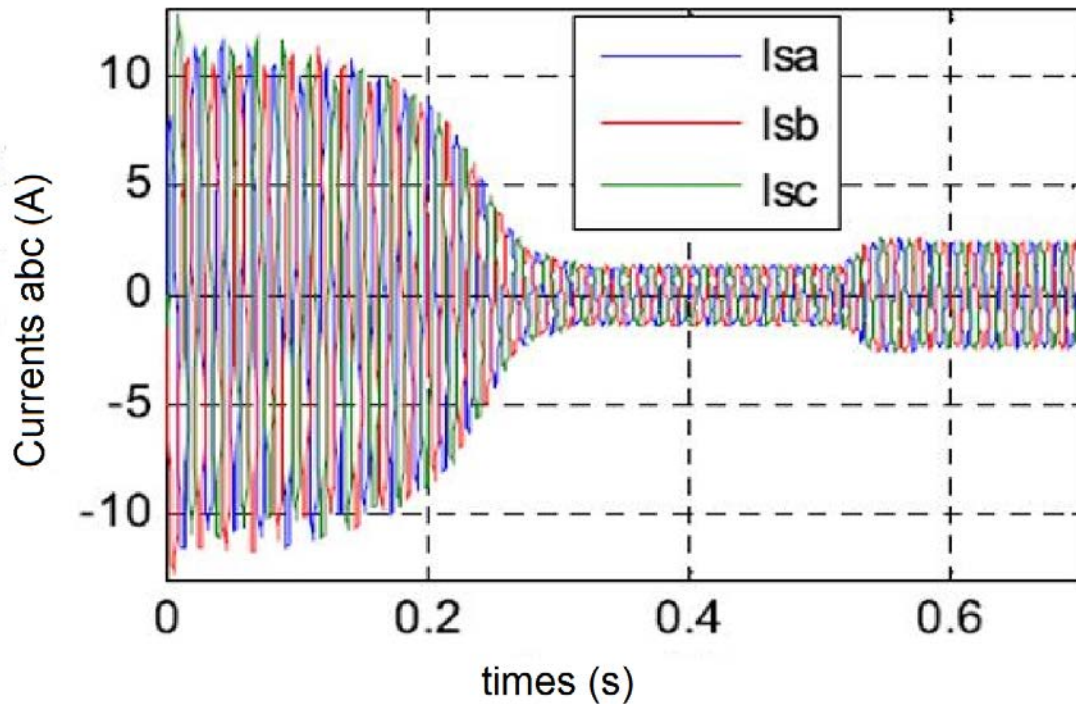


**Figure III.3:** Evolution of currents in the three-phase

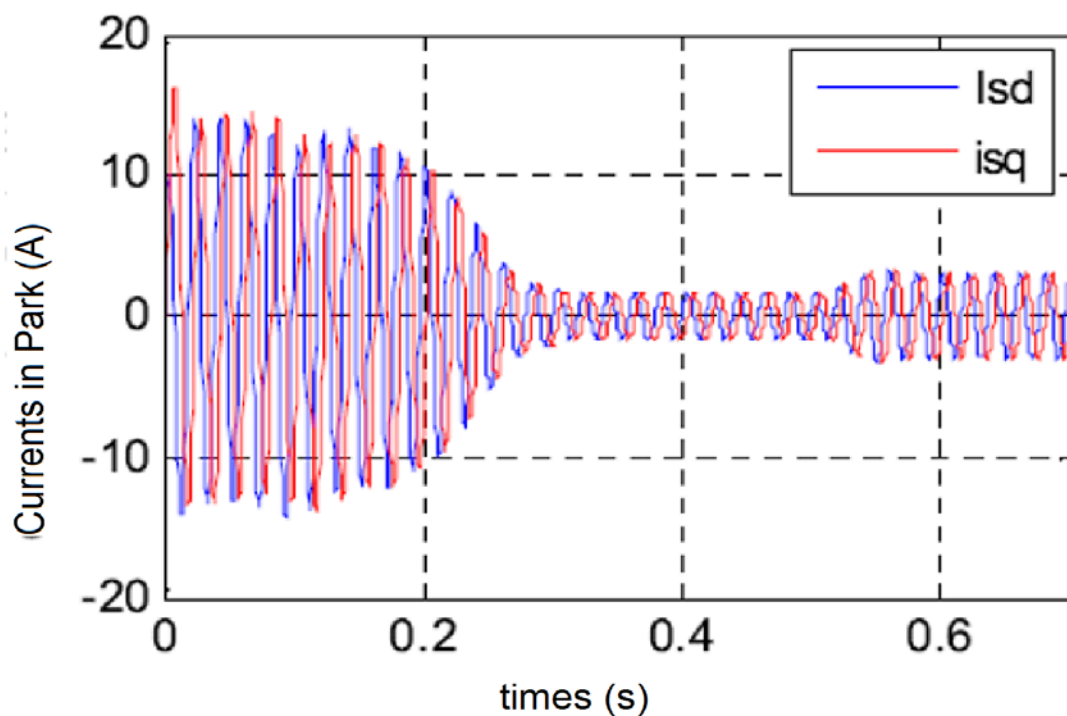


**Figure III.4:** Evolution of currents in the two-phase

Since an electromechanical torque is needed to get the induction machine up to speed, it draws a lot of current when it first starts.

The machine currents in the Park frame, both with and without a load, are in quadrature of the same maximum value, as shown in **Figures (III.2) and (III.4)**.

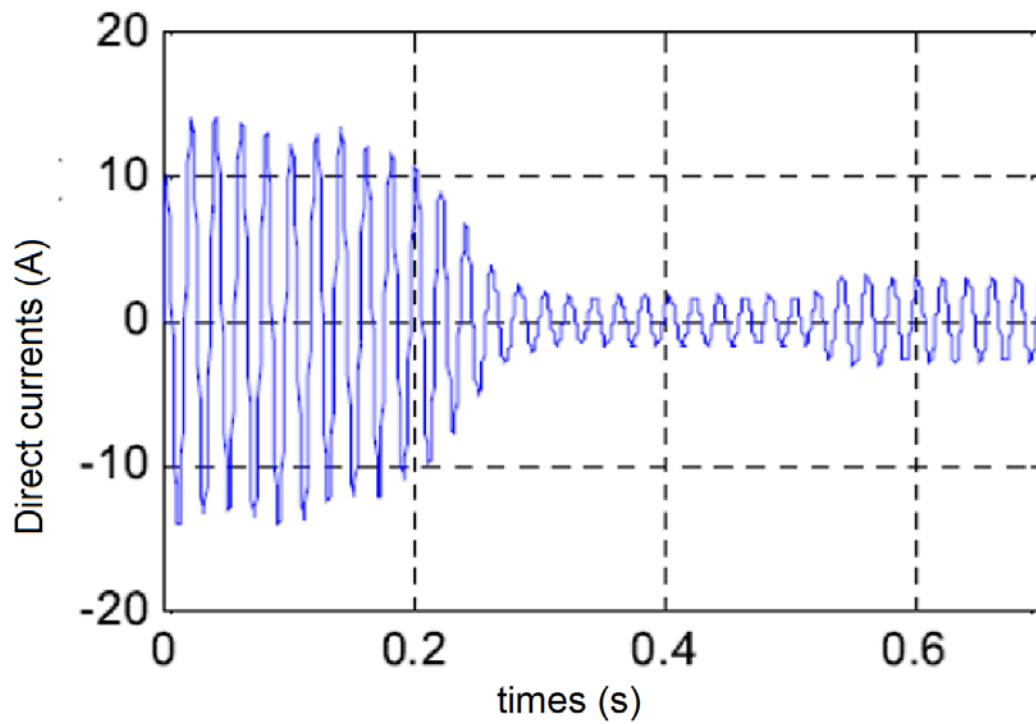


**Figure III.5:** evolution of direct.

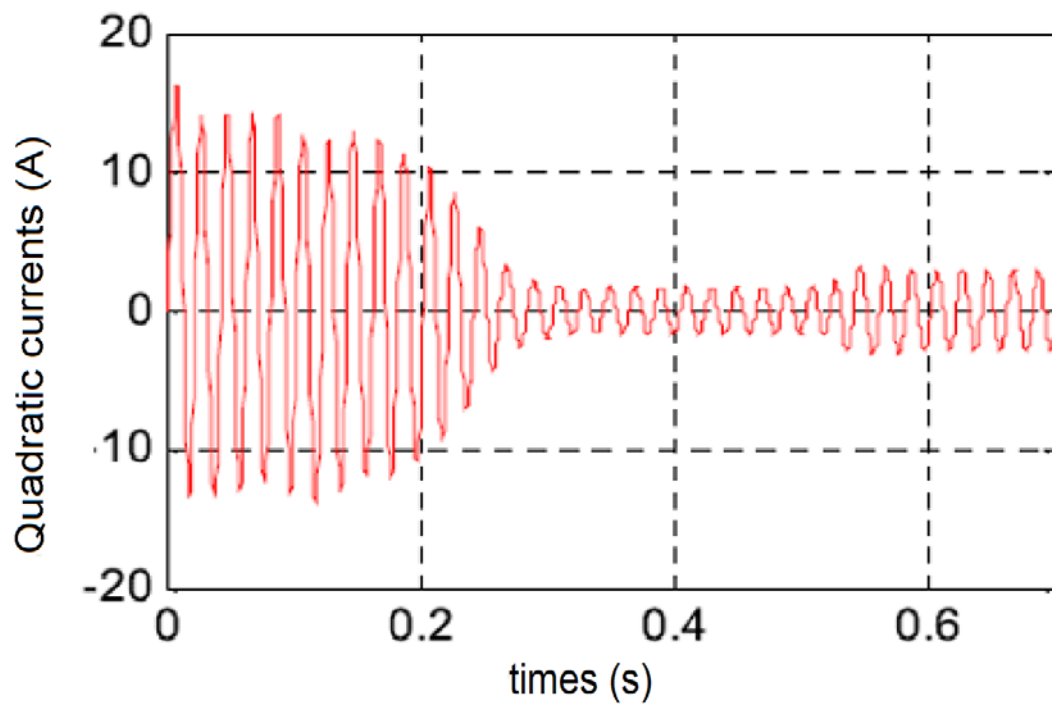


**Figure III.6:** evolution of quadratic currents.



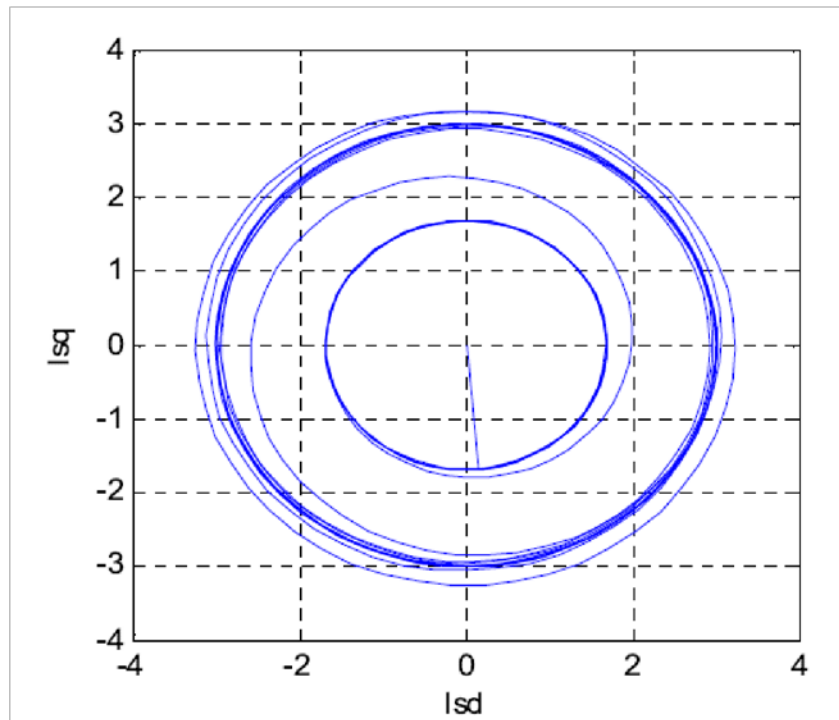


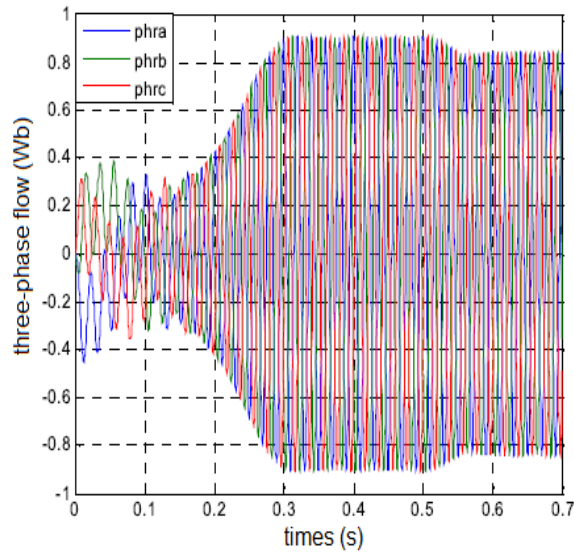
**Figure III.7:** Phase plane of direct and quadrature currents.

The curves form a trajectory in the  $isd-isq$  plane, illustrating how the direct and quadrature components of the current evolve over time

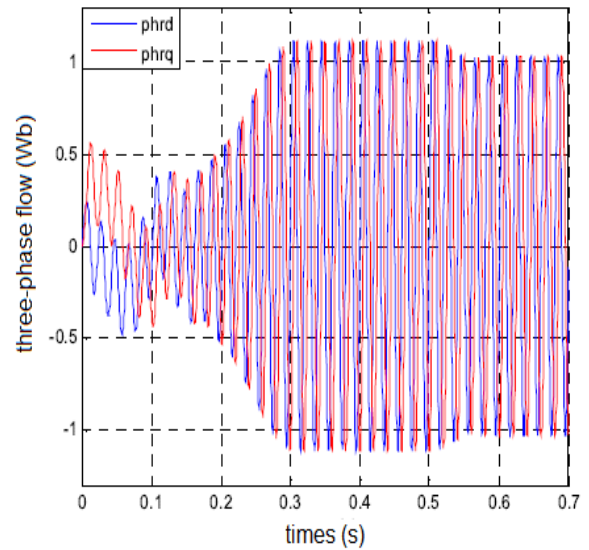
Behavior of the curves:

The curves appear as concentric loops or spirals, indicating cyclical or oscillatory behavior of the currents in the Park frame.

**Figure (III.4)** illustrates how a balanced induction machine would operate in the absence of faults. The inner circle displays the quadrature current as a function of the direct current of the fault-free induction machine without the application of load torque in its permanent regime, while the outer circle displays the same function in the presence of the load torque.



(a)



(b)

**Figure III.8:** Rotor flow in both frames

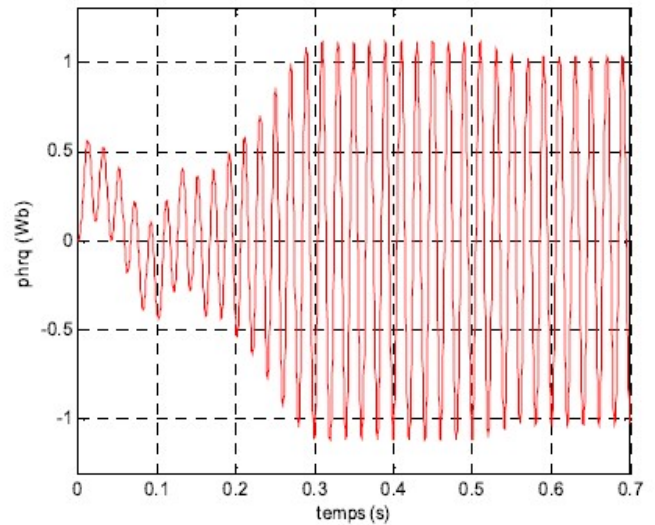
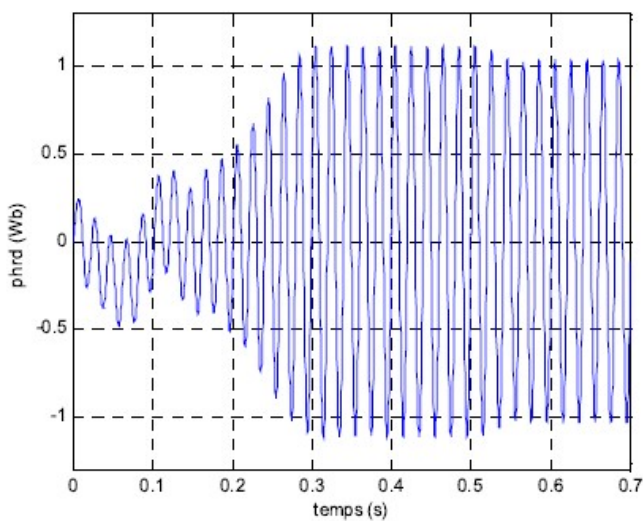


**Figure III.9:** induction machine's rotor flow in the Park frame.

This images show two plots analyzing the rotor flux in both the three-phase (abc) frame and the Park's (dq) frame over time.(**Figure III.8**)

Plot (a): Rotor Flux in the Three-Phase (abc) Frame

The plot shows the rotor flux components for the three phases (phra, phrb, phrc) over time. Initially, all three phase fluxes exhibit oscillatory behavior with increasing amplitude, indicating a transient response

Around 0.3 seconds, the oscillations stabilize, and the fluxes exhibit a periodic steady-state oscillation, reflecting the steady-state operation of the rotor flux in the three-phase system.

### Plot (b): Rotor Flux in Park's (dq) Frame

The plot shows the rotor flux components in the dq frame over time

Similar to Plot (a), both  $\phi_{rd}$  and  $\phi_{rq}$  show initial oscillatory behavior with increasing amplitude, indicating a transient response.

Around 0.3 seconds, these fluxes stabilize and exhibit periodic steady-state oscillation.

The alignment and oscillatory nature in both components indicate how the dq transformation captures the dynamic behavior of the rotor flux.

These plots are crucial for understanding the behavior of rotor flux in electric machines. The three-phase frame provides insight into individual phase fluxes, while the Park's frame helps in analyzing the system in a rotating reference frame, simplifying the control and analysis of induction machine.

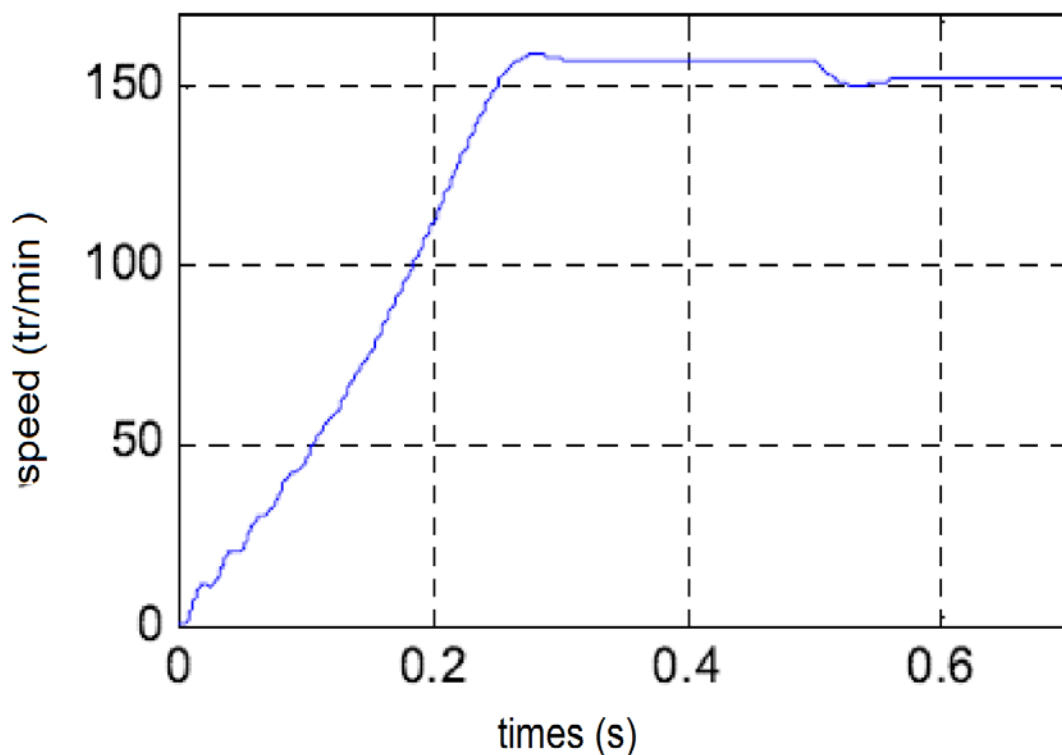


**Figure III.10:** The Evolution of mechanical speed

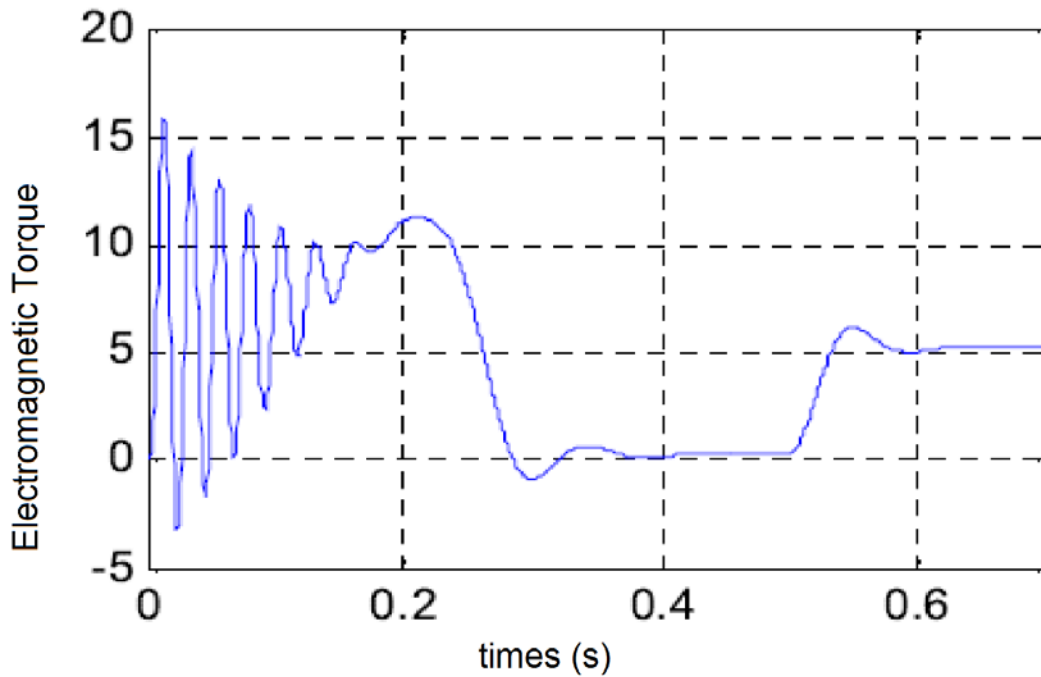


**Figure III.11:** The Evolution of electromagnetic torque

The noise produced by the mechanical part in transient mode can be explained by the intense pulsation of the electromagnetic torque. After the load torque is applied, the torque tends toward a value near zero, which represents the friction torque (the machine runs empty), and it will attempt to balance it.

When the torque of the load is applied, the speed (**Figure III.10**) drops.

### III.1.3 Unbalanced three-phase power supply

There are two ways that the voltage imbalance manifests itself: either there is a decrease in the voltage amplitude or one or more phases are completely absent.

Equation (4.2) provides the supply voltage to be employed in the first scenario.

$$U_S = \begin{bmatrix} 200\sqrt{2}\sin(2\pi ft) \\ 220\sqrt{2}\sin\left(2\pi ft + \frac{2\pi}{3}\right) \\ 220\sqrt{2}\sin\left(2\pi ft - \frac{2\pi}{3}\right) \end{bmatrix} \quad (4.2)$$

The progression of the tensions depicted in the Park reference frame is seen in (**Figure III.12**).

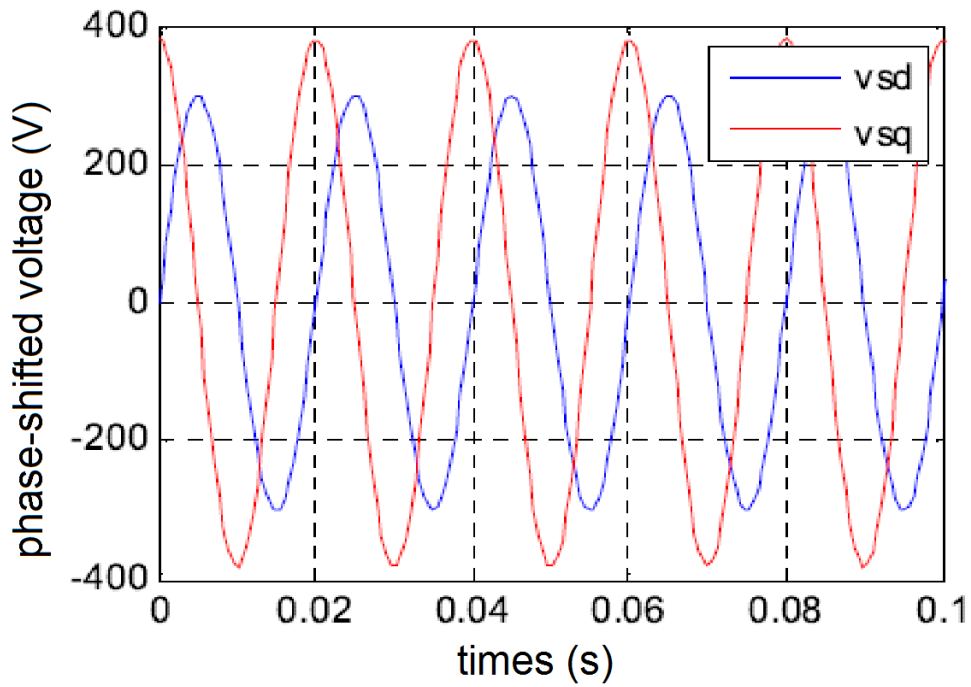


**Figure III.12:** Evolution of imbalanced voltages

The two direct and quadrature phases' amplitudes are not equal, and the voltage in the Park reference frame is out of balance.

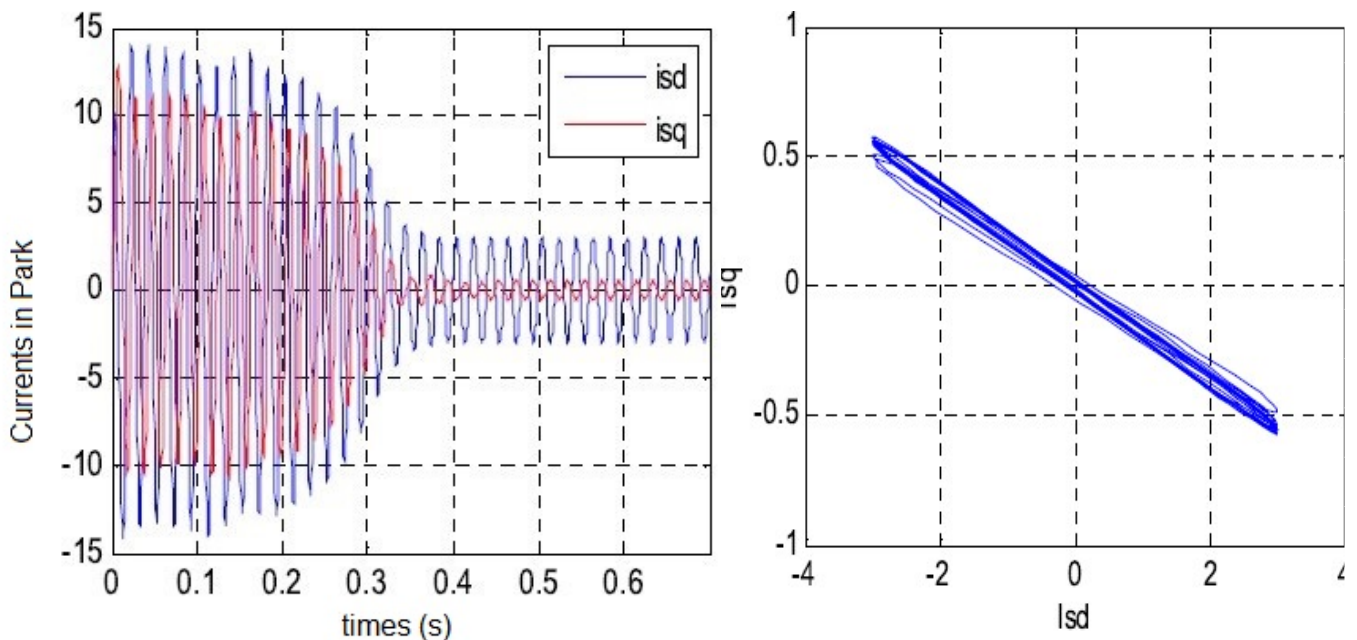


**Figure III.13. :** Current in Park.

The currents are unbalanced in the case of unbalance of the supply voltage, this is clear in the maximum values of the two currents in Figure (3.13).a and in the deformation of the circle giving the phase plane

### Current in Park's Frame Under Voltage Imbalance :

The image consists of two plots (a) and (b) related to the analysis of current in the Park's transformation frame (also known as the dq0 transformation) under voltage imbalance conditions.

The additional information highlights the effects of supply voltage imbalance on the currents.

#### Detailed Analysis :

Plot (a): This plot shows the time-domain response of two currents,

The currents are unbalanced due to the supply voltage imbalance.

Initially, both  $i_{sd}$  and  $i_{sq}$  exhibit significant oscillations with high maximum values, indicating a transient response due to the imbalance.

Around 0.3 seconds, the oscillations dampen and the currents stabilize, indicating the system reaches a steady state.

The maximum values of the currents during the initial period reflect the severity of the imbalance.

Plot (b):Phase Plane of  $i_{sd}$  ,  $i_{sq}$

This plot is a phase plot showing the relationship between  $i_{sd}$  and  $i_{sq}$

The deformation of the circle in the phase plane indicates voltage imbalance

Instead of a perfect circle, the plot forms a distorted ellipse with a negative slope, showing the coupling between  $i_{sd}$  , $i_{sq}$

The deformation suggests that the imbalance in the supply voltage significantly affects the direct and quadrature axis currents.

The plots in the image effectively illustrate the effects of voltage imbalance on the currents in the Park's transformation frame. The time-domain plot (a) shows how the currents respond dynamically to the imbalance, with high initial oscillations that dampen over time. The phase plane plot (b) reveals the imbalance through the deformation of the circle, providing a clear visual indicator of the coupling and interaction between  $i_{sd}$  and  $i_{sq}$  These analyses are crucial for diagnosing and understanding voltage imbalances in electrical systems, aiding in the design of effective control and mitigation strategies.

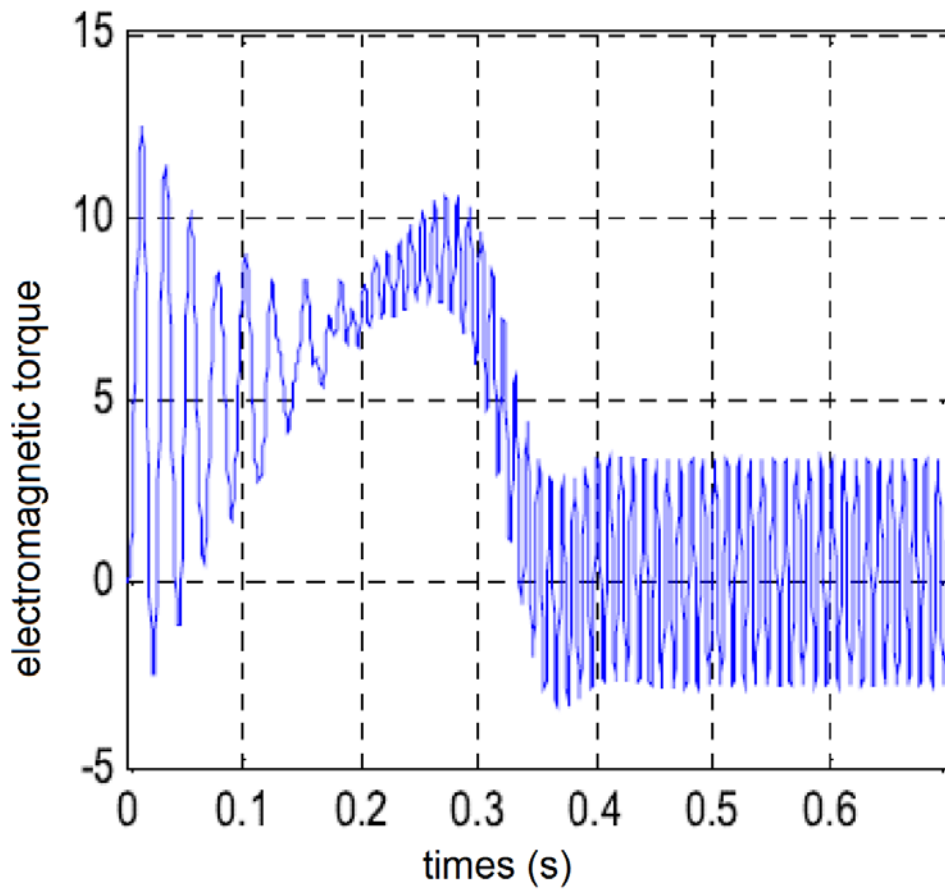


**Figure III.14** : Evolution of torque

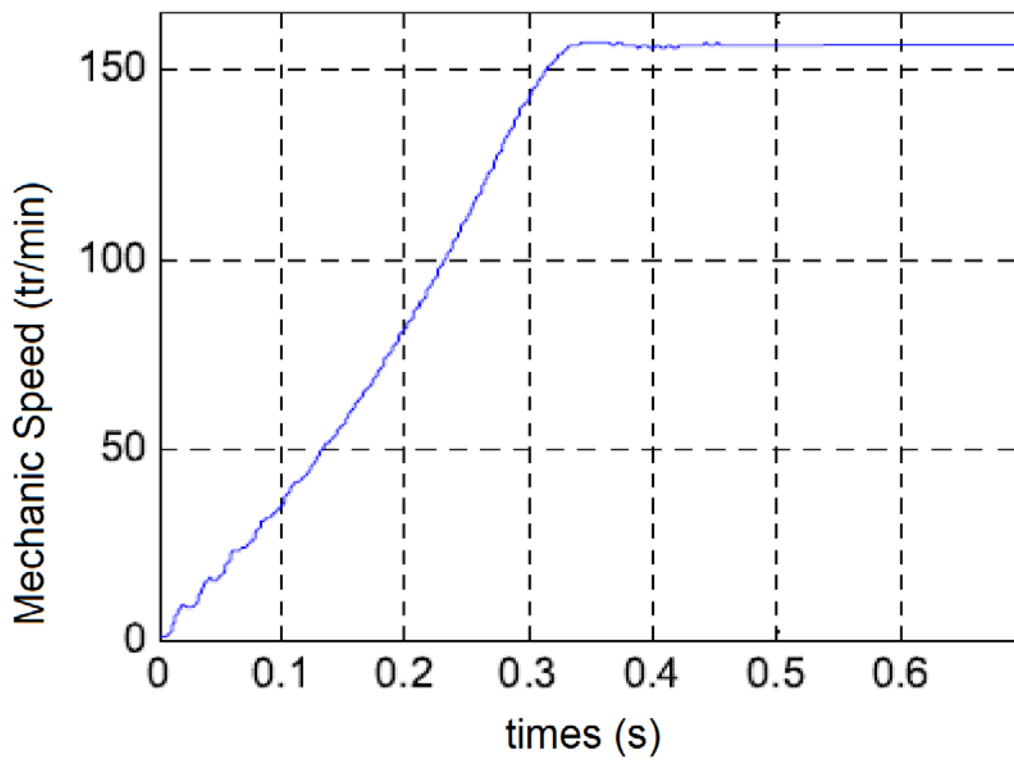


**Figure III.15** : Evolution of speed

When there are supply voltage imbalance faults, the electromagnetic torque oscillates. The machine's inertia filters the mechanical speed.

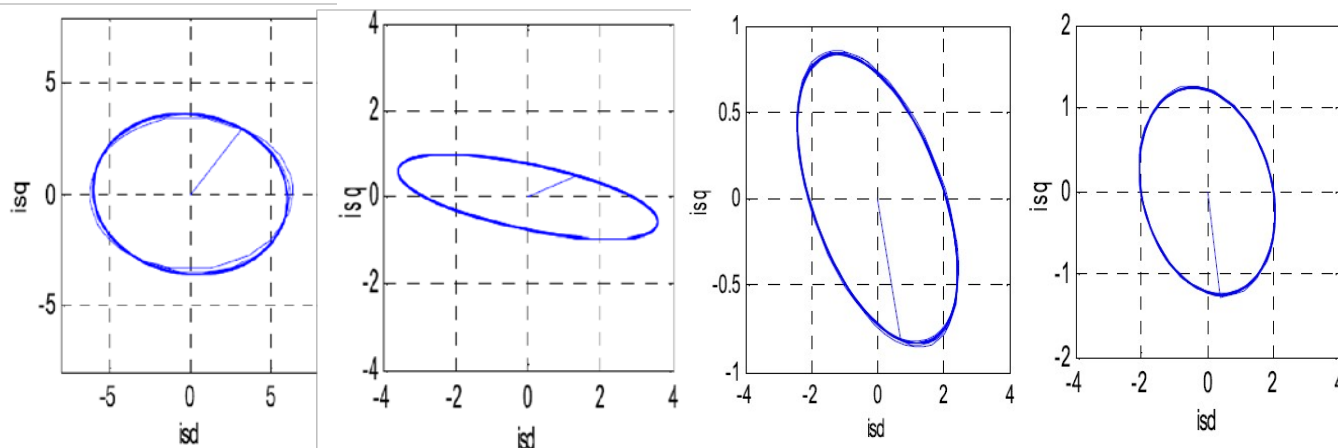


**Figure III.16:** Function  $I_{sd} = f(I_{sq})$  under various voltage imbalance situations.

The images illustrate the function  $I_{sd} = f(I_{sq})$  under different voltage imbalance conditions, showing how the direct-axis current ( $I_{sd}$ ) and the quadrature-axis current ( $I_{sq}$ ) are related in these situations. These plots are useful for understanding the impact of voltage imbalances on the currents in an electrical machine or system.

Detailed Analysis of Each Plot:

Plot (a): Phase A receives no power at all.

The plot shows an ellipse centered at the origin with its major axis tilted.

The shape indicates a coupling between  $I_{sd}$  and  $I_{sq}$  due to the voltage imbalance.

Plot (b): The voltage ratio is 54.55%.

This plot displays a narrower ellipse, which is also tilted.

The narrow shape suggests a stronger coupling between  $I_{sd}$  and  $I_{sq}$  indicating a significant imbalance.

Plot (c): The voltage ratio is 81.82%.

The plot shows an upright ellipse with its major axis aligned vertically.

The vertical alignment indicates that the voltage imbalance is primarily affecting  $I_{sq}$  more than  $I_{sd}$ .

Plot (d): The voltage ratio is 90.91%.

This plot displays an ellipse that is less elongated and has its major axis tilted.

The moderate elongation and tilt indicate a balanced coupling but with both  $I_{sd}$  and  $I_{sq}$  being affected by the voltage imbalance.



The plots illustrate how voltage imbalances affect the relationship between  $I_{sd}$  and  $I_{sq}$  under different conditions. By analyzing the shape and orientation of the ellipses, one can gain insights into the nature and severity of the voltage imbalances, using the phase plane of direct and quadrature currents as an effective indicator.

### III.2- Simulation of an induction machine with faults

The induction machine becomes unbalanced when a fault occurs on one of its phases. In this instance, the intern-turn short-circuits fault is on phase A when the MAS is powered by a balanced voltage and speed measurement at first, and it is not present when the MAS is controlled without speed measurement.

#### III.2.1 Balanced voltage supply

In this instance, the machine is driven by a balanced network. The machine's state variables are displayed over time in. At time  $t=0.4s$ , the machine has a reduction defect of 10 % of turns on phase A, at time  $t=0.9s$ , this fault increases to 14 %. It is expected that the speed is quantified.

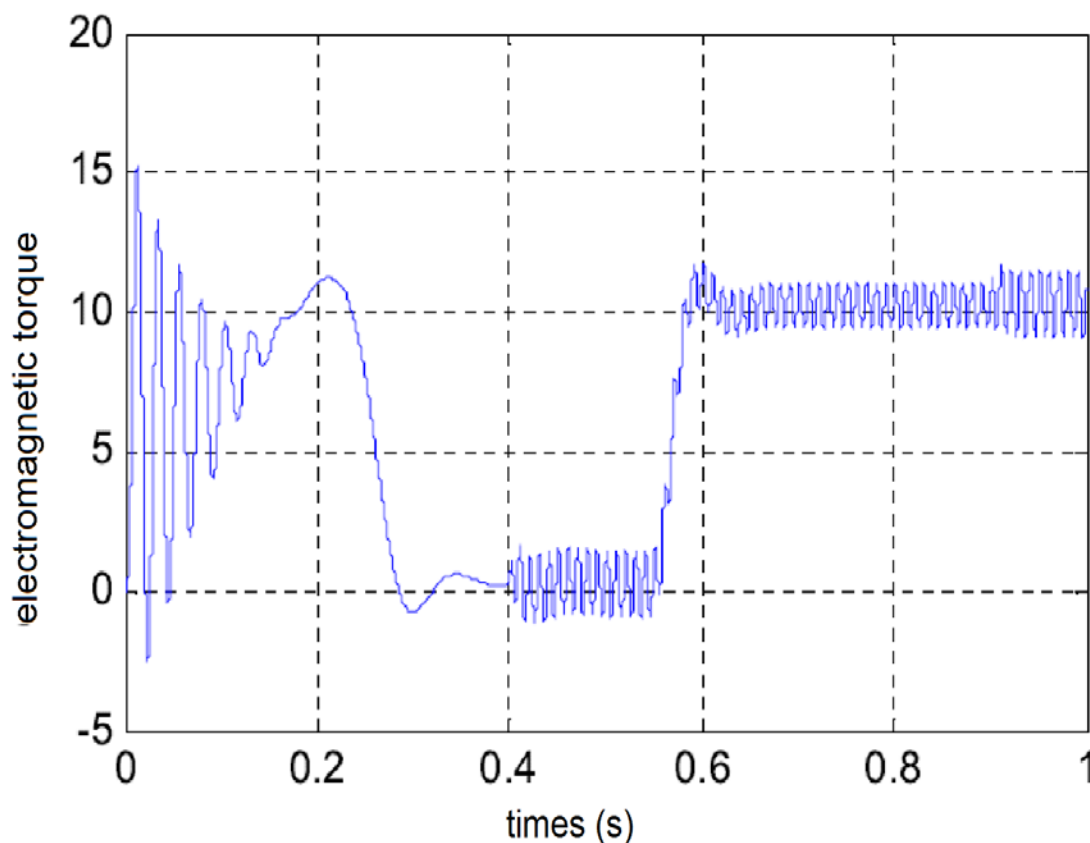


Figure III.17: Electromagnetic couple

Initial behavior (0 to 0.4s):

the torque oscillates and stabilizes around a certain value. This initial period might represent normal operation with minor fluctuations due to inherent system dynamics or initial disturbances.

At  $t=0.4s$ :

there is a sudden reduction of 10% in the number of turns on phase A, indicative of an intern-turn short-circuits fault affecting the phase. This reduction decreases the effective turns in the winding, altering the inductance and causing a disturbance in the electromagnetic torque.

The graph shows a noticeable dip in the torque around this time, followed by oscillations as the system tries to stabilize. The intern-turn short-circuits fault affects the magnetic flux distribution and the current in phase A, leading to these observed oscillations.

Intermediate Behavior(0.4 to 0.9s)

the system seems to reach a new quasi-steady state, but with superimposed oscillations. This suggests that the machine is operating under the altered conditions caused by the 10% reduction in turns.

At  $t=0.9s$ :

the fault severity increases, and the reduction in the number of turns on phase A increases to 14%. This further disturbs the system, as evidenced by another sudden change in the torque profile.

The torque again shows a significant disturbance and increased oscillations. The fault's escalation increases the asymmetry in the magnetic field and current distribution, causing more pronounced oscillations and disturbances in the torque.

Final Behavior(0.9 to 1s):

After the fault severity increases at  $t=0.9s$  the system again attempts to stabilize under the new conditions. The torque oscillations are more prominent compared to the previous state, indicating the machine's struggle to maintain stable operation under the increased fault conditions.

The graph illustrates how intern-turn short-circuits faults in an electrical machine's phase windings affect the electromechanical torque. The machine experiences significant disturbances in the torque whenever there is a change in the severity of the fault, showing its dynamic response to the altered electrical characteristics caused by the reduction in the number of turns due to the fault.

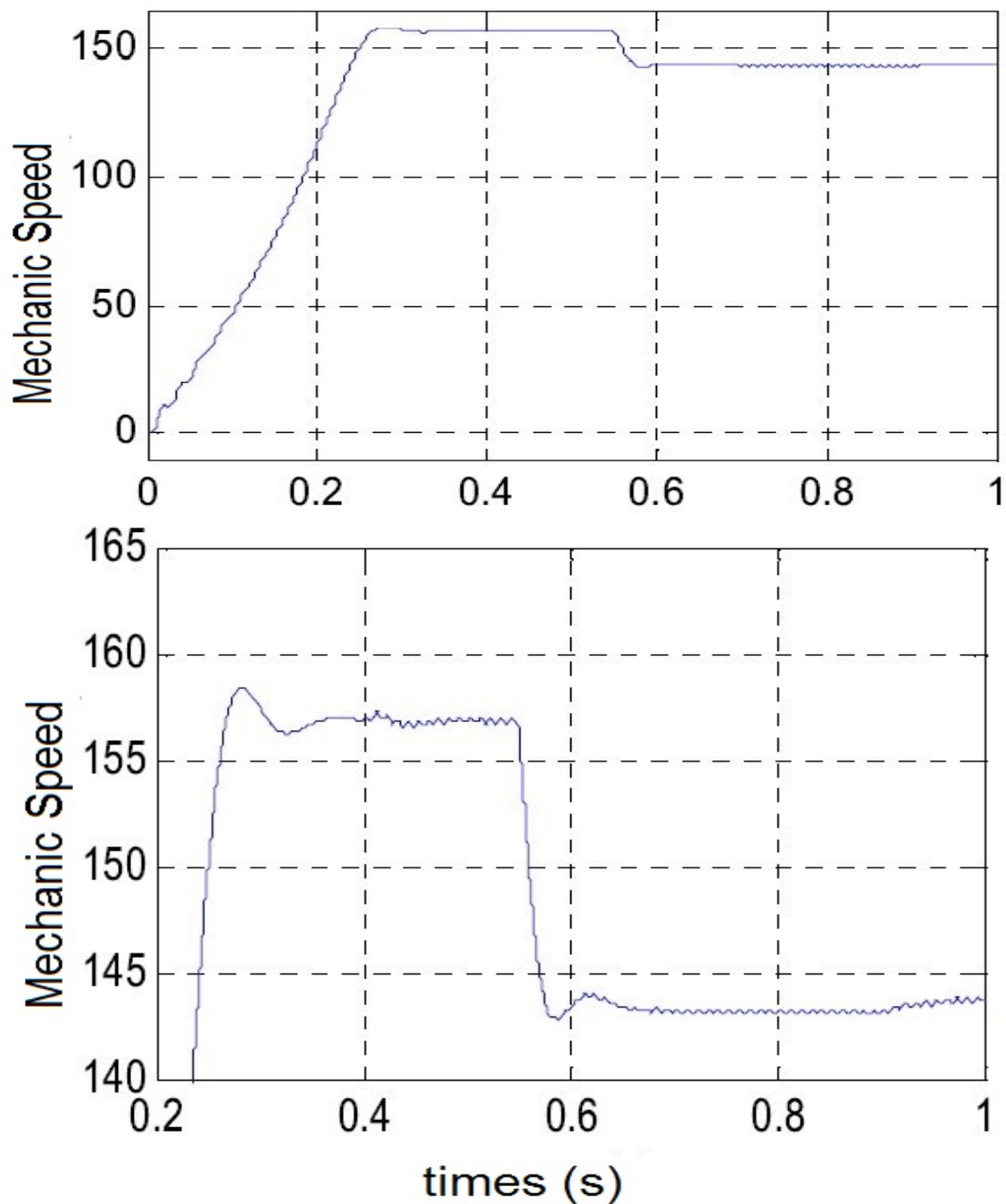


**Figure III.18:** (a) mechanical speed, (b) zoom speed.

These graphs show the mechanical speed (*vitesse mécanique*) of the electrical machine as a function of time (*temps*). The two subfigures provide different views of the speed data: (a) shows the overall mechanical speed, while (b) provides a zoomed-in view of the speed around the critical times of interest. in light of the intern-turn short-circuits fault affecting phase A:

Graph (a): Overall Mechanical Speed

Initial speed:

From  $t=0$  to  $t=0.4s$ , the mechanical speed increases smoothly from 0 to around 150 units.

This phase represents the normal acceleration of the machine as it reaches its operating speed.

At  $t=0.4s$ :

there is a noticeable drop in speed. This corresponds to the 10% reduction in the number of turns on phase A due to an inter-turn short-circuits fault.

The sudden reduction in turns affects the torque generated by the machine, which in turn reduces the mechanical speed.

Intermediate Steady-State (0.4 to 0.9 seconds):

Between  $t=0.4$  and  $t=0.9s$ , the machine stabilizes at a new, slightly lower speed. This is the new steady-state operating speed under the altered conditions caused by the fault

At  $t=0.9s$  :

there is another drop in speed, corresponding to an increase in the fault severity (14% reduction in turns on phase A).

This further affects the torque and hence the mechanical speed, causing another reduction Final

Stabilization(0.9 to 1s):

the machine stabilizes at an even lower speed, reflecting the increased severity of the fault.

Graph (b): Zoomed-In Mechanical Speed

This graph provides a closer look at the mechanical speed around the times of interest.

Speed Fluctuations at  $t=0.4s$ :

there is a dip in speed followed by oscillations. This detailed view shows the immediate impact of the 10% reduction in turns on phase A. The system experiences fluctuations as it attempts to stabilize at the new operating condition.

Speed Fluctuations at  $t=0.9s$  :

the graph shows another dip followed by oscillations, indicating the response to the increased fault severity (14% reduction in turns on phase A).

The machine's speed drops and oscillates as it adjusts to the new fault condition.

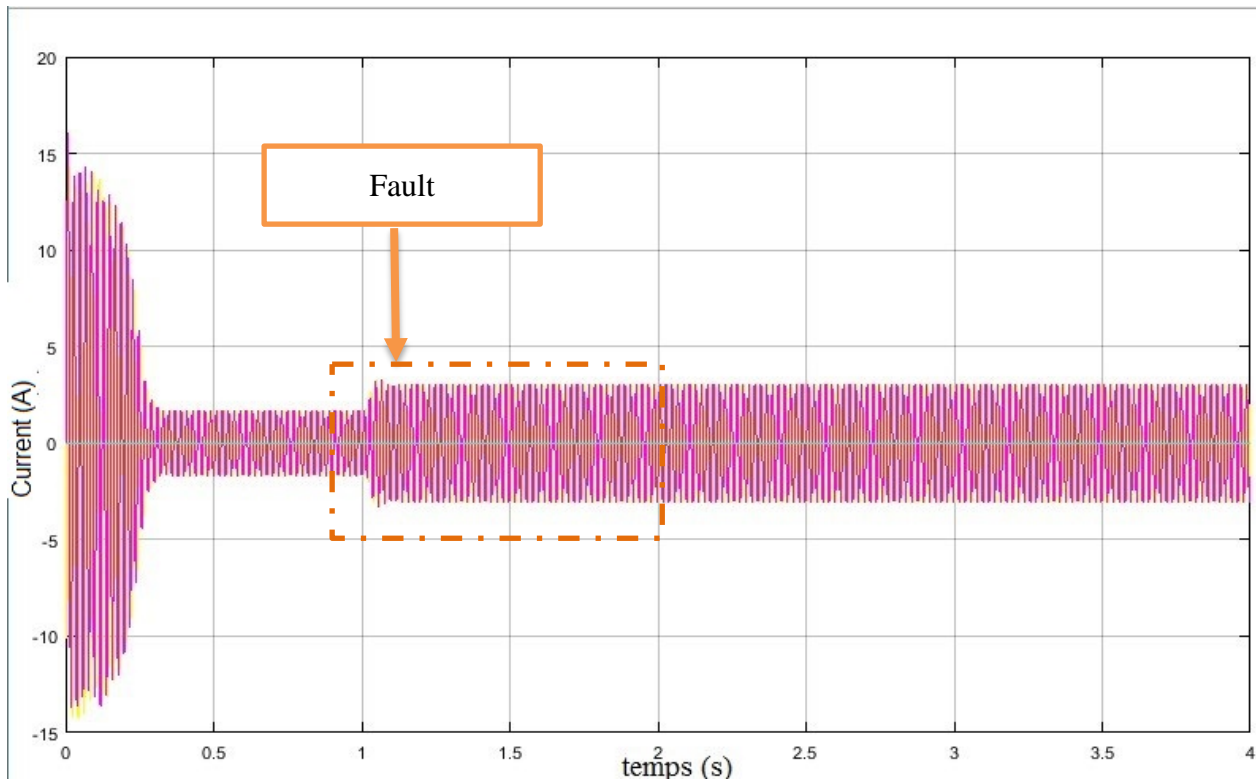


**Figure III .19** Phase A stator current.

**Initial Behavior:**

the currents exhibit oscillatory behavior with decreasing amplitude, indicative of the machine stabilizing from initial conditions. The oscillations reduce in magnitude, suggesting the system is approaching a steady state under normal operating conditions.

**At t=1s :**

At approximately t=1s, there is a significant and abrupt change in the current waveform. This change indicates the occurrence of a intern-turn short-circuits fault.

The currents show an immediate alteration in their pattern, characterized by increased amplitude and more pronounced oscillations. This is consistent with the introduction of a fault that causes a sudden imbalance in the current distribution.

**Post-Fault Behavior (after t=1s):**

After the fault occurs, the currents exhibit persistent oscillations with a higher frequency and amplitude compared to the pre-fault condition. This is a typical response to a intern-turn short-circuits fault, where the electrical parameters of the machine (such as inductance and resistance) are altered. The oscillatory behavior indicates that the machine is operating in a disturbed state, attempting to cope with the fault. The fault creates asymmetry in the magnetic field, resulting in unbalanced currents and increased oscillations.

The graph clearly shows a distinct change in the current behavior at this time, which aligns with the occurrence of a fault. The increased amplitude and oscillations of the currents post-fault reflect the machine's disturbed operation and attempt to stabilize under the new faulty conditions.

## **Conclusion**

The Main case of this chapter is to use an observer to solve the three-phase asynchronous machine's fault detection problem. Intern-turn intern-turn short-circuits in the stator turns are the problem at hand. Since observability is a need for observer synthesis, the three-phase asynchronous machine's observability was next investigated using the various models created in chapter 2. This demonstrated the unobservability of the machine asynchronous model stated in the three-phase reference. This is because rotor quantity information is lacking. Conversely, the model improves in relation to the flaws, which are recorded in the Park reference frame. On the basis of this model, a sliding mode observer was synthesized.

The suggested method demonstrates a very high detection capacity and enables the creation of a residual fault detection that is resistant to changes in the load torque and supply voltage. Three residues serve as the foundation for fault isolation, which is accomplished by logical combination. The suggested insulation technique performs worse when failures happen on two or three phases at once. Conversely, in the event of a single phase malfunction, the insulation functions flawlessly. In the following chapter, the susceptibility of the residual generator to parametric fluctuations will be investigated. We will also talk about how valid the models created in Chapter 2 are.

## General Conclusion

The work presented in this thesis focuses on fault diagnosis applied to three-phase induction machines. Stator turns intern-turn short-circuits are the faults taken into consideration. An analytical model and observer technique was chosen. This provides the benefit of operating online concurrently with the system under observation. Using the signals from this system and the ones the observer has reconstructed, a residual generator is created. It makes fault locating and detection possible.

The three-phase induction machine is a good option in many applications at fixed or variable speed because of its intriguing qualities, which include resilience, low cost, and ease of assembly. However, simplifying assumptions (symmetry, periodicity, magnetic linearity) are made during its classical modeling. Then, the intricate electromagnetic processes occurring there (space harmonics, saturation, influence of notches, etc.) are not considered in detail. When a fault occurs, the induction machine's symmetry is changed (intern-turn short-circuits of stator turns, static and dynamic eccentricity, etc.); the traditional models that were created as a result are no longer appropriate to explain how the machine operates when in fault mode. The problems can be handled by the models that result from considering the induction machine's geometric topology and constituent parts. However, these models typically demand the knowledge of construction-related factors that are not supplied by the machine's producers. The demands of real-time fault detection cannot be met by their exorbitant calculation times. These different modeling-related limitations have encouraged the creation of techniques for induction machine diagnosis that rely on external measurements.

These considerations have led us to direct our work towards the development of models dedicated to diagnosis:

- making sure intern-turn short-circuits failures in the stator turns are taken into consideration.
- appropriate for use with analytical model-based diagnostic techniques.

Due to the induction machine's symmetry changing when a stator turn intern-turn short-circuits fault occurs, the resistance and inductance matrices had to be redefined, and three coefficients that quantified the faults had to be added in order to create these new models. This helped us develop the first model that explained how the induction machine functions while it is in fault mode. The notation used to write this model is known as multiplicative form. Additional development is done using an approximation. The second model came from this computation. Faults are represented in this second model as an independent input vector that is applied to the system. In terms of flaws, this form is referred to as affine. We then proposed a third model, which was derived by transforming the previous model using the Park transformation, based on considerations based on the observability conditions of the induction machine. The latter is more appropriate for applying analytical redundancy techniques, specifically the observer-based approach, which has been kept in place. Online flaw detection is one of

this approach's primary benefits. It also enables you to reap the rewards of the laborious work done in the synthesis and application of observers.



## References

1. Zwingelstein G., «Diagnostic des défaillances. Théorie et pratique pour les systèmes industriels ». Traité des nouvelles technologies - série Diagnostic et Maintenance 1995. Editions HERMES.
2. Venkatasubramanian V., Rengaswamy R., Yin K. and Kavuri S. N., «A review of process fault detection and diagnosis. Part I: Quantitative model-based methods». Computer and Chemical Engineering 27, (2003), pp 293-311.
3. Isermann R. « Model-based fault detection and diagnosis- status and applications >>. Annual Reviews in Control 29 (2005), 71-85 p.
4. Kinnaert M. « Fault diagnosis based on analytical models for linear and non linear systems-A Tutorial ». SAFEPROCESS 2003, Washington, D.C.USA, (June 9-11-2003), 37-50 p.
5. Hofling T. and Iserman R. «Adaptive parity equations and advanced parameter estimation for fault detection and diagnosis»> Proc. Of the 13<sup>th</sup> IFAC World congress, San Francisco, USA, (A996), 50-60 p.
6. Floquet T., Barbot J.P., Perruquetti W. and Djamaï M., «On the robust fault detection via sliding mode disturbance observer». International Journal of Control, (10 may 2004), V. 77, 622 629 p.
7. Alcorta Garcia E. and Frank P. M., «Fault detection and isolation in non linear systems». Proc. of ECC'99, (31 august 3september 1999), Karlsruhe, Germany.
8. De Persis C. and Isidori A., «A geometric approach to non linear fault detection and isolation». IEEE Trans. on Automatic Control, V. 46. N°. 6,(June 2001).
9. Djamaï M., Barbot J.P. and Bthoux O., «On the problem of fault detection and residual generation», Proc. of the IEEE CDC (2000), Australia.
10. Gertler J., «Fault Detection and Isolation Using Parity Relations»>.Control Engineering Practice, 5, (1997), 635-661 p.
- 11.Chow E. Y. and Wilsky A.S., «Analytical redundancy and the design of robust failure detection systems», IEEE Trans. on Automatic Control, V.29,N°7, (1984), 603-614 p.
- 12.-Frank P.M., « Fault diagnosis in dynamics systems using analytical and knowledge-base redundancy». Automatica, V. 26, N°3, 459-474p., (1990).
- 13.- Alcorta Garcia E. and Frank P. M., «A novel design of structured observer-based residuals for». Proc. of American Control Conference, California, USA, (June 1999), 1341-1345p.
- 14.Frank P.M., Scherier G. and Alcorta Garcia E., «Non linear observer for fault detection and isolation». Lecture Notes in Control and Information Science, 244, (1999), 400-422p.
15. Marques Cardoso A.J., Cruz S.M. and Fonseca D. S. B., «Intern-turn Stator Winding Fault Diagnosis in Three-Phase Induction Motor, by Park's Vector Approach». IEEE Transaction on Energy Conversion, V. 14, N° 3, (September 1999), 595-598p.

16. Nedjari H. and Benbouzid M. E. H., «Monitoring and Diagnosis of Induction Motors Electrical Faults Using a current Park's Vector Pattern Learning Approach». IEEE Transaction on Industry Application, V. 36, N° 3,(May/June 2000), 730-735 p.
17. Benbouzid M. E. H., «A Review of Induction Motors Signature Analyses as Medium of Faults Detection». IEEE Transactions on Industrial Electronics, V. 47, N°5, (October 2000), 984-993 p.
18. Nandi S. and Tolyat H.A., «Novel frequency-domain-based technique to detect stator intern-turn faults in induction machines using stator induced voltages after switch-off». IEEE Transactions on Industry Application, V. 38, N°1, (January/February 2002).
19. Zhengja H., Jiyuan Z., Yibin H. and Qingfeng M., «Wavelet transform and multi-resolution signal decomposition for machinery monitoring and diagnosis» in IEEE International Conference on Industrial Technology, (ICIT'96), (1996), 724-727 p.
20. Da Silva A. A., «Rotating machinery monitoring and diagnosis using short-time Fourier transform and Wavelet techniques». Proc. Int. Conf. Maintenance Rel., V. 1, Knoxville, TN, USA, (1997), 1401-1415 p.
21. Kohler J. L., Sottile J. and Trutt F. C., «Condition Monitoring of Stator Windings in Induction Motors: Part I- Experimental Investigation of the Effective Negative-sequence Impedance Detector». IEEE Trans. on Ind. App., V. 38, N°5, (Sep/Oct 2002), 1447-1453 p.
22. Ferdjouni A., Salhi H., DjemaI M. and Busawon K., «Observer-based detection of intern-turn intern-turn short-circuit in three phase induction motor stator windings», The Mediterranean Journal of Measurement and Control, V. 2, N° 3,(2006).
23. Devanneaux V., «Modélisation de la machine asynchrone triphasé à cage d'écureuil en vue de la surveillance et du diagnostique», Thèse Doctorat, INP Toulouse, France, (2002).
24. Benbouzid M. E. H., Vieira M. and Theys C., "Induction motor's faults detection and localization using stator current advanced signal processing techniques" IEEE Transaction on Power Electronics, Vol. 14, N° 1, pp 14 - 22, January 1999
25. Thomson, W.T.; Fenger, M. "Industrial application of current signature analysis to diagnose faults in 3-phase squirrel cage induction motors" Pulp and Paper Industry Technical Conference, 2000. Conference Record of 2000, pp 205-211
26. Jearance N., Raison B., Sename O., « Observer based detection and isolation in induction machine drive», Proceeding of the IFAC Safeprocess (2000), Budapest, Hungary, 955-960.
27. Ferdjouni A., « Diagnostic des defaults à l'aide d'observateurs, application à la machine asynchrone », Thèse Doctorat d'état, Université de Blida, Algérie, (2007).
28. M. O. Mahmoudi, << Sur la commande de la machine asynchrone alimentée en tension», Thèse de doctorat d'état, ENP Alger 1999.

29. Boumegoura T., « Recherche des signatures électromagnétiques des défauts dans une machine asynchrone et synthèse d'observateurs en vue du diagnostique », Thèse Doctorat, Université de Lyon, France, (2001).
30. Kennedy, J., Eberhart, R.: "Particle swarm optimization". In: Proc. of IEEE International Conference on Neural Networks, IEEE Press (1995) 1942-1948
31. Kennedy J.: Stereotyping: "Improving particle swarm performance with cluster analysis". In: Proc. of the IEEE Congress on Evolutionary Computation. (2000) 1507-1512.
- 32-O. V. Thorsen and M. Dalva «Failure Identification and Analysis for High-Voltage Induction Motors in the Petrochemical Industry». IEEE Transactions On Industry Application, Vol. 35, NO. 4, (July / August 1999).
- 33- Bonnett A. H., «Root Cause AC Motor Failure Analysis with a Focus on Shaft Failures». IEEE Transactions on Industry Application, Vol. 36, NO 5, (September/October 2000).
- 34-Stone G. and Kapler J., «Stator winding monitoring». IEEE Industry Application Magazine, (September/October 1998).
- [35] Application de la technique de linéarisation par retour d'état à la commande d'une machine asynchrone ". PFE, Université M'sila, 2003
- ([36] S. Mendaci différentes stratégies du contrôle direct du couple d'un moteur a induction associées à un observateur de flux par modes de glissement"" ,thèse de magister, université de batna. (2003).) (
- [37] F. Zidani (1996)"" étude comparative par simulation numérique d'un pilotage vectorielle et scalaire d'une machine à induction alimenté par un onduleur a MLI"" , thèse de magister en électricité industrielle, université de Batna.)
- [38]: HAKIMA CHERIF « Détection des défauts statorique et rotorique dans la machine asynchrone en utilisant l'analyse par FFT et ondelettes », Mémoire de Magistère, Université de Biskra, sep 2014.
- [39]: Bousseksou Modélisation analytique des machines Asynchrone application au diagnostic. Mémoire de Magister. Université Mentouri Constantine. Algérie 2007
- [40]: : A. Menacer, "Contribution à l'identification des paramètres et des états d'une machine à induction pour diagnostic et développement de commande robuste : robustesse vis-à-vis de défauts", Thèse de doctorat, Université de Batna, Décembre 2007
- [41]: BELHAMDI SAAD« Diagnostic des défauts de la machine asynchrone contrôlée par différents techniques de commande », Thèse de doctorat Université de Biskra Mai 2014
- [42]:GILLES HOUDOUIN « Contribution à la modélisation de la machine asynchrone en présence de défauts rotoriques », Thèse de doctorat université de havre mai 2004.
- [43]: Sobczyk T. J. and Izvorski A., "Recognition of rotor eccentricity of induction motor based on the fourier spectra of phase currents" Proc. ICEM'98, pp 408-413, Vol 1, september 2-4 1998 Istanbul Turkey

# Appendix A

coefficients of the state matrices of the healthy MAS of the park mark

$$\alpha_1 = \frac{-4R_s L_r x^2 - 12R_s L_r M - 9M^2 R_s - 9M^2 R_r}{(3M + 2L_r) + (3L_s M + 2L_r L_s + 3L_r M)}$$

$$\alpha_2 = \frac{6M R_r}{(3M + 2L_r) + (3L_s M + 2L_r L_s + 3L_r M)}$$

$$\alpha_3 = \frac{3M}{(3L_s M + 2L_r L_s + 3L_r M)}$$

$$\alpha_4 = \frac{3M R_r}{(3M + 2L_r)}$$

$$\alpha_5 = \frac{-2R_r}{(3M + 2L_r) + (3L_s M + 2L_r L_s + 3L_r M)}$$

$$b_1 = \frac{3M + 2L_r}{(3L_s M + 2L_r L_s + 3L_r M)}$$

MAS model linked to the rotating field

in a reference frame linked to the rotating field we have () and the model given in equation (2.34) becomes:

$$\frac{d}{dt} \begin{bmatrix} I_{sdqo} \\ \Phi_{rdqo} \end{bmatrix} = \begin{bmatrix} \frac{-lstr + M^2 sr R_r}{\sigma l s l r^2} & 0 & \frac{R_r M}{\sigma l s l r^2} & p\Omega \\ 0 & \frac{-lstr + M^2 sr R_r}{\sigma l s l r^2} & -p\Omega & \frac{R_r M}{\sigma l s l r^2} \\ \frac{R_r M}{l r} & 0 & -\frac{R_r}{l r} & -p\Omega \\ 0 & \frac{R_r M}{l r} & p\Omega & -\frac{R_r}{l r} \end{bmatrix} \begin{bmatrix} I_{sdqo} \\ \Phi_{rdqo} \end{bmatrix} + \begin{bmatrix} \frac{1}{\sigma l s} & 0 \\ 0 & \frac{1}{\sigma l s} \end{bmatrix} [Us]$$

$$\sigma = 1 - \frac{M^2}{l s l r} ,$$

coefficient of the MAS state matrices with presence of turns short-circuit fault

$$\alpha_1 = \frac{-R_s L_r M + L_s (3M + 2L_r)}{L_s (3M L_r + L_s (3M + 2L_r))}$$

$$\alpha_2 = \frac{-6R_r L_s M^2}{L_s (3M L_r + L_s (3M + 2L_r)) (3M + 2L_r)}$$

$$\alpha_3 = \frac{-R_s L_r M}{(3L_s M + 2L_r L_s + 3L_r M)}$$

$$\alpha_4 = \frac{3R_r L_s M^2}{L_s (3M L_r + L_s (3M + 2L_r)) (3M + 2L_r)}$$

$$\alpha_5 = \frac{2M R_r}{L_s (3M L_r + L_s (3M + 2L_r)) (3M + 2L_r)}$$

$$\alpha_6 = \frac{\sqrt{3}M}{(3MLr) + Ls(3M + 2Lr)}$$

$$\alpha_7 = \frac{-RrM}{(3M + 2Lr)}$$

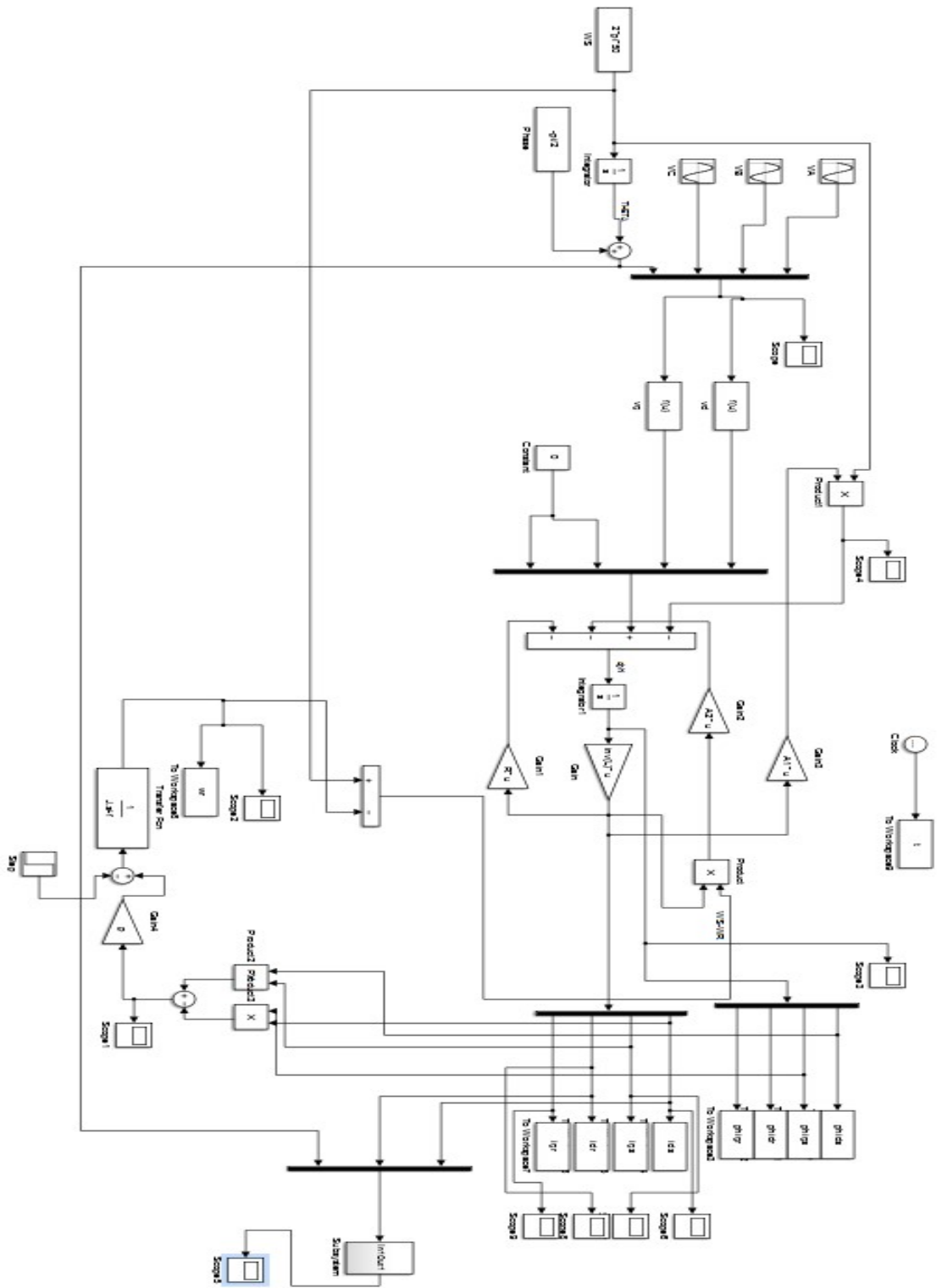
$$\alpha_8 = \frac{-RrM + 2lr}{lr(3M + 2Lr)}$$

$$\alpha_9 = \frac{-RrM}{lr(3M + 2Lr)}$$

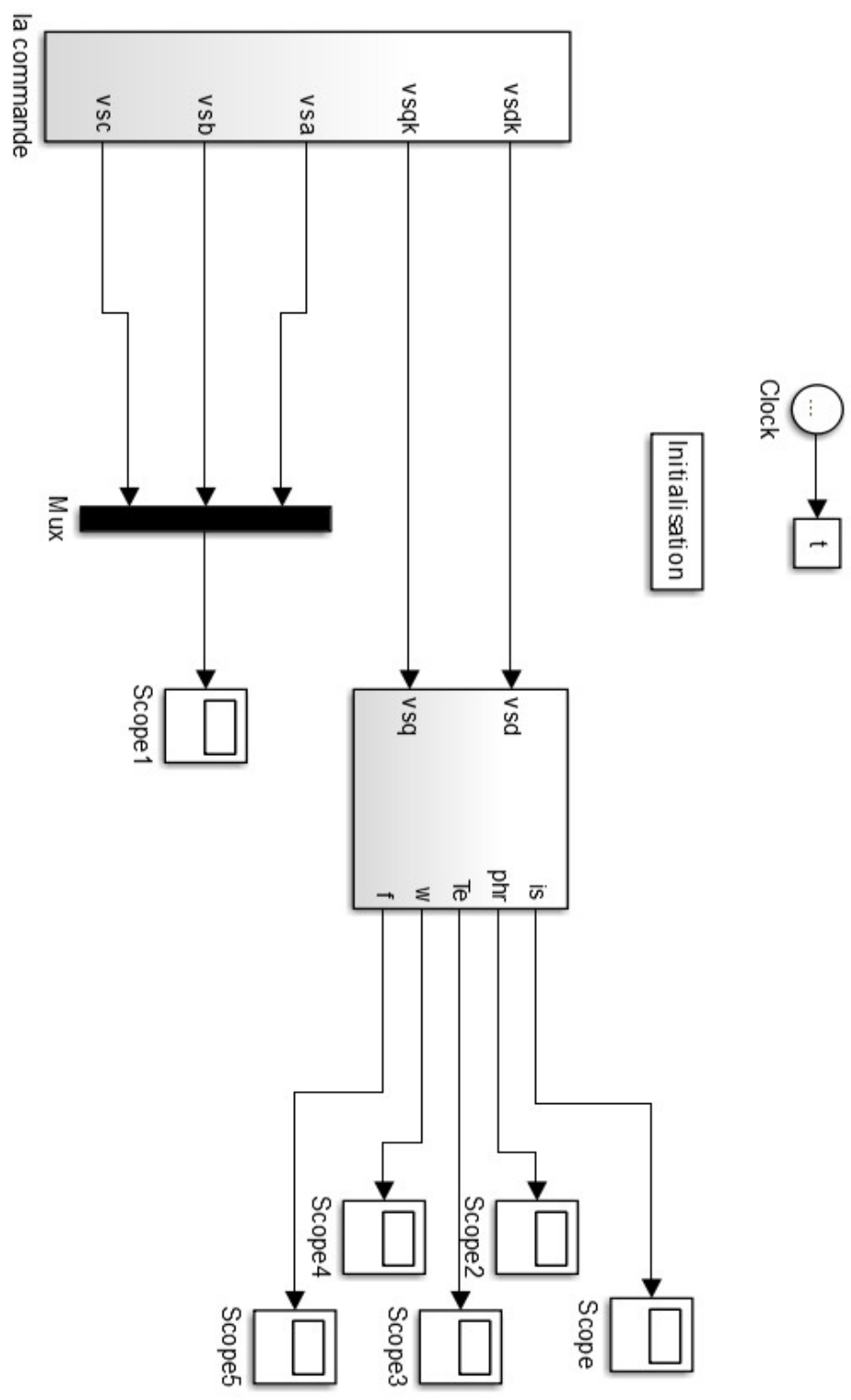
$$b_1 = \frac{Mlr + ls(3M + 2lr)}{Ls(3MLr + Ls(3M + 2Lr))}$$

$$b_2 = \frac{Mlr}{Ls(3MLr + Ls(3M + 2Lr))}$$

# Appendix B



# Appendix C



# Appendix D

Induction machine parameters

$$R_r=4.85$$

$$R_s=10.04$$

$$M=0.44H$$

$$I_{s\sigma} = 0.0566H$$

$$I_{r\sigma} = 0.017H$$

$$J=0.0135Nm^2$$

$$f_v=0.0135Nm^2S^{-1}$$

$p=2$  pairs of poles





غرداية في: .....

## إذن بالطباعة (مذكرة ماستر)

بعد الاطلاع على التصحيحات المطلوبة على محتوى المذكرة المنجزة من طرف الطلبة التالية أسماؤهم:

1. الطالب (ة): حجاج بن الدين

2. الطالب (ة): باكلي محمد

تخصص:

ننح نحن أعضاء لجنة المناقشة:

الإمضاء	الصفة	المؤسسة الأصلية	الرتبة	الإسم واللقب
	المتحن 1	جامعة غرداية	MAA	Kada Biter
	المتحن 2	جامعة غرداية	MAA	Boumedienne LAADJAL
	المؤطر	جامعة غرداية	McB	Abdessalam Kifouche
	رئيس اللجنة	جامعة غرداية	PR	Abdelmadjid Kaddour

الإذن بطباعة النسخة النهائية لمذكرة الماستر الموسومة بعنوان:

Modeling induction machine with inter-  
turn short circuit

